

Multi-field Inflation in High-Slope Potentials

Vikas Aragam^a Sonia Paban^a Robert Rosati^a

^aTheory Group, Department of Physics, University of Texas at Austin, Austin, TX 78712, USA

E-mail: aragam@utexas.edu, paban@physics.utexas.edu, rjrosati@utexas.edu

Abstract. We present two families of multi-field potentials that support inflation while satisfying the refined de Sitter and the distance swampland conjectures. Both families feature Planck-compatible phenomenology. The first is a helix-type potential, in a flat field-space metric, that satisfies the conjectures via a high turning rate. This model has a tensor-to-scalar ratio close to, but below, the current experimental limits and small non-gaussianities. The second family, an example of orbital inflation, utilizes a negatively curved field metric to achieve prolonged inflation with nontrivial turning in the presence of a tachyonic direction. Although perturbations in this model undergo an exponential growth before horizon exit, it is always possible to match the measured amplitude of the power spectrum by lowering the scale of inflation if the turning rate is low enough. We identify a Planck-compatible region of parameter space in which the scale of inflation is above that of nucleosynthesis. Due to the rapid growth, this model predicts an exponentially suppressed value for the tensor-to-scalar ratio.

ArXiv ePrint: [1905.07495](https://arxiv.org/abs/1905.07495)

UTTG-05-19

Contents

1	Introduction	1
2	Notation	2
2.1	Perturbations	2
3	Helix-trajectory potentials	3
3.1	Background dynamics	6
3.2	Perturbations	8
4	Superpotential model	10
5	Conclusions	18
6	Acknowledgements	18
A	Steady-state solution to helical potential	19
B	Transport Method	21
C	Derivation of Superpotential Model	23
D	Derivation of Geodesics	25

1 Introduction

In multi-field models it is possible to have both a period of inflation and a steep potential [1–3]¹. In these models the ratio of the gradient of the potential to the potential is still proportional to the rate of time evolution of the Hubble parameter, but the proportionality coefficient can be much larger than one:

$$\epsilon_V \simeq \epsilon_H \left(1 + \frac{\omega^2}{9H^2} \right), \quad \epsilon_V = \frac{M_{Pl}^2}{2} \left(\frac{|\nabla V|}{V} \right)^2, \quad \epsilon_H = -\frac{\dot{H}}{H^2}. \quad (1.1)$$

Here ω (called Ω in some references) measures the turning rate of the trajectory, and it has been assumed that ϵ_H and $|\eta_H| \ll 1$. The relation (1.1) is a statement about the background field motion. It is the first step toward a viable inflation model, but fitting the experimental data will impose further constraints both on the classical trajectory (number of e-folds) and on the quantum fluctuations: n_s , r , isocurvature power and non-gaussianities. It is known that models of multi-field inflation can produce sizable isocurvature power whenever $\omega \neq 0$ for some field masses [12–15]. It is also known that they can be unstable [16]. For these reasons it is important to build and analyze actual models.

In this paper we construct potentials with large values of $\epsilon_V \gtrsim 1$, both in flat and negatively curved field-space geometries, and probe their compatibility with the experimental limits. More precisely, the examples below satisfy the constraint [17]

$$\epsilon_V \gtrsim 1 \quad \text{or} \quad \eta_V \lesssim -1 \quad (1.2)$$

$$\eta_V \equiv M_{Pl}^2 \times \text{minimum eigenvalue}(V_{,IJ})/V$$

in a region of field space of magnitude $\Delta\phi \gtrsim M_{Pl}$, where $\Delta\phi$ is the geodesic distance in field-space. The two examples we provide will illustrate that imposing compatibility with CMB data significantly reduces the parameter space that satisfies (1.1). The possibility of generating inflation in potentials with these properties is intriguing in view of the swampland conjectures [17–22]², though the approach followed in this paper is bottom-up. In fact, we lack a compelling reason to expect a top-down approach to generate the combination of metric and potential of the examples that we analyze.

Hyperinflation [3] is an interesting idea that balances large potential gradients against the (negative) curvature of field space to generate a period of inflation. Negative curvature field-space metrics appear frequently in string theory compactifications. The second family of solutions we present in this work uses the same field-space metric as Hyperinflation but a different potential. The follow-up work to the initial Hyperinflation proposal has focused on its quantum fluctuations [157]. In particular, [16, 158–160] have pointed out that the perturbations experience an exponential growth before horizon exit due to the rapid turning trajectory and the negatively curved field space. This is not fatal as long as the turning rate is low enough [49, 161]. Further work by Bjorkmo and Marsh [43, 57] has generalized the idea of hyperinflation to models with more than two fields and a broader class of potentials.

The two families of potentials analyzed in this paper are distinct from hyperinflation, but create similarly strong non-geodesic inflationary trajectories. The helix-type potential

¹See [4–11] for exploring alternative ways of making inflation compatible with steep potentials.

²For a follow-up on the cosmological consequences of the conjectures, see [2, 11, 18–21, 23–156]. An interesting possibility is that the conjectures are a consequence of forbidding eternal inflation [23].

assumes a flat field space metric and is hence clearly different from hyperinflation. The second family is a particular example of orbital inflation [59, 162] which assumes the same negatively curved field space as hyperinflation but has a different potential. Its perturbations face similar challenges to hyperinflation. As we will explain in section 4, this model has a region of parameter space for which the refined swampland constraints are compatible with current experimental data. As in hyperinflation, these solutions lead only to experimentally compatible results when inflation happens at very low scales. A measurement of the metric perturbations in the near future would rule out this family of models as realizations of inflation that are compatible with the refined swampland conjectures.

2 Notation

Before describing our models, a quick note on notation. We consider models with N_f scalar fields in $(3+1)$ spacetime dimensions and Friedman-Lemaître-Robertson-Walker metric, with spacetime metric signature $(-, +, +, +)$. The field-space has a metric $\mathcal{G}_{IJ}(\phi^I)$. Greek letters label space-time indices, lower-case Latin letters label spatial indices and upper-case Latin letters label field-space indices, $I, J = 1, 2, \dots, N_f$. We work in units where the reduced Planck mass is set to one, but occasionally insert it in expressions to make dimensions apparent.

With these assumptions the equations of motion for the background fields are:

$$\mathcal{D}_t \dot{\phi}^I + 3H \dot{\phi}^I + \mathcal{G}^{IJ} V_{,J} = 0 \quad (2.1)$$

where $V_{,I} \equiv \mathcal{D}_I V$. The covariant derivative with respect to cosmic time is defined as:

$$\mathcal{D}_t A^I \equiv \dot{\phi}^J \mathcal{D}_J A^I = \dot{A}^I + \Gamma_{JK}^I A^J \dot{\phi}^K. \quad (2.2)$$

As these two equations show, it is possible to offset large gradients in the potential against curvature to have slow-roll inflation.

2.1 Perturbations

This section largely follows the notation of [163]. The evolution of the perturbations is given by:

$$\mathcal{D}_t^2 Q^I + 3H \mathcal{D}_t Q^I + \left[\frac{k^2}{a^2} \delta_J^I + \mathcal{M}_J^I - \frac{1}{a^3} \mathcal{D}_t \left(\frac{a^3}{H} \dot{\phi}^I \dot{\phi}_J \right) \right] Q^J = 0 \quad (2.3)$$

where Q^I are the Mukhanov-Sasaki variables. They are gauge invariant with respect to space-time gauge transformations to first order in the perturbations. The mass-squared matrix appearing in the equation of motion for the perturbations is

$$\mathcal{M}^I{}_J \equiv \mathcal{G}^{IK} (\mathcal{D}_J \mathcal{D}_K V) - \mathcal{R}_{LMJ}^I \dot{\phi}^L \dot{\phi}^M \quad (2.4)$$

where \mathcal{R}_{LMJ}^I is the Riemann tensor for the field-space manifold. We may decompose the perturbations along directions tangent (adiabatic: Q_σ) and perpendicular (entropic: δs^I) to the classical trajectory:

$$\begin{aligned}
Q_\sigma &\equiv \hat{\sigma}_I Q_I = \frac{\dot{\sigma}}{H} \mathcal{R}_c, \quad \text{where} \quad \hat{\sigma}^I \equiv \frac{\dot{\phi}^I}{\dot{\sigma}}, \quad \dot{\sigma}^2 \equiv \mathcal{G}_{IJ} \dot{\phi}^I \dot{\phi}^J \\
\delta s^I &\equiv \hat{s}_J^I Q^J, \quad \hat{s}^{IJ} \equiv \mathcal{G}^{IJ} - \hat{\sigma}^I \hat{\sigma}^J \\
\omega^I &\equiv \mathcal{D}_t \hat{\sigma}^I = -\frac{1}{\dot{\sigma}} V_{,K} \hat{s}^{IK} \quad \omega = |\omega^I|.
\end{aligned}$$

Here, \mathcal{R}_c is the gauge invariant curvature perturbation. The equation for the adiabatic mode is:

$$\ddot{Q}_\sigma + 3H\dot{Q}_\sigma + \left[\frac{k^2}{a^2} + \mathcal{M}_{\sigma\sigma} - \omega^2 - \frac{1}{a^3} \frac{d}{dt} \left(\frac{a^3 \dot{\sigma}^2}{H} \right) \right] Q_\sigma = 2 \frac{d}{dt} (\omega_J \delta s^J) - 2 \left(\frac{V_{,\sigma}}{\dot{\sigma}} + \frac{\dot{H}}{H} \right) (\omega_J \delta s^J). \quad (2.5)$$

This indicates that there is a particular combination of entropic modes with special physical significance ($\omega_J \delta s^J$). To separate this combination from the rest, one introduces a unit vector that points in the direction of the turning rate:

$$\hat{s}^I \equiv \frac{\omega^I}{\omega}, \quad \gamma^{IJ} = G^{IJ} - \hat{\sigma}^I \hat{\sigma}^J - \hat{s}^I \hat{s}^J \quad (2.6)$$

$$\delta s^I = \hat{s}^I Q_S + B^I \quad \text{where} \quad Q_s \equiv \hat{s}_J Q^J, \quad B^I \equiv \gamma^I_{\ J} Q^J. \quad (2.7)$$

The evolution of Q_s is given by the equation:

$$\ddot{Q}_s + 3H\dot{Q}_s + \left[\frac{k^2}{a^2} + \mathcal{M}_{ss} + 3\omega^2 - \Pi^2 \right] Q_s \quad (2.8)$$

$$= 4 \frac{k^2 \omega}{a^2 \dot{\sigma}} \Psi - \mathcal{D}_t (\Pi_J B^J) - \Pi_J \mathcal{D}_t B^J - \mathcal{M}_{IJ} \hat{s}^I B^J - 3H (\Pi_J B^J) \quad (2.9)$$

where $\Pi^I = \frac{1}{\omega} \mathcal{M}_{KJ} \hat{\sigma}^K \gamma^{IJ}$, $\mathcal{M}_{ss} \equiv \mathcal{M}_{IJ} \hat{s}^I \hat{s}^J$, and

$$\frac{k^2}{a^2} \Psi = \frac{\dot{H}}{H} \left[\frac{d}{dt} \left(\frac{H}{\dot{\sigma}} Q_\sigma \right) - \frac{2H\omega}{\dot{\sigma}} Q_s \right]. \quad (2.10)$$

Taking the sub- and super-horizon limits respectively, the evolution of Q_s becomes:

$$0 = \ddot{Q}_s + 3H\dot{Q}_s + \begin{cases} \left(\frac{k^2}{a^2} + \mathcal{M}_{ss} - \omega^2 \right) Q_s - 4 \frac{\omega}{\dot{\sigma}} \frac{\dot{H}}{H} \frac{d}{dt} \left(\frac{H}{\dot{\sigma}} Q_\sigma \right) & \text{if } k^2 \gg (aH)^2 \\ \left(\mathcal{M}_{ss} + 3\omega^2 \right) Q_s & \text{if } k^2 \ll (aH)^2 \end{cases} \quad (2.11)$$

We denote the entropic mode's effective super-horizon mass in two-field inflation as $\mu_s^2 \equiv \mathcal{M}_{ss} + 3\omega^2$ and the effective sub-horizon mass as $\mu_{s,sub}^2 \equiv \mathcal{M}_{ss} - \omega^2$.

3 Helix-trajectory potentials

In this section we present a class of three-field helix-like potentials in flat field-space with a high turning rate, a large ϵ_V , and observationally consistent phenomenology.

Different potentials with helix-type behavior have been studied before in [59, 164, 165]. However, all of them are two-field models and none of them support high-slope inflation with $\epsilon_V \gtrsim \mathcal{O}(1)$. Other differences include: trajectories following the minima of Dante’s Inferno [164] produce no turning. Spiral Inflation produces turning [165] but has a tachyonic mode and a growing radius. The potential presented below is single-valued while the example of Shift-symmetric Orbital Inflation in [59] is multi-valued and has an additional shift symmetry which guarantees a flat direction in the potential. We later analyze an instance of orbital inflation in section 4.

The helical potential described here is the first flat field space construction to locally satisfy the dS conjecture and produce observationally consistent phenomenology. This potential forces a helical trajectory in field space. There are three fields, x, y, z , with canonical kinetic terms.

$$V = \Lambda^4 \left(e^{z/R} + \Delta \left(1 - \exp \left[\frac{-(x - A \cos z/f)^2 - (y - A \sin z/f)^2}{2\sigma^2} \right] \right) \right) \quad (3.1)$$

The potential is exponential in z/R , other than a gaussian divot curled into a helix with radius A and period $2\pi/f$. The depth and width of the divot are set by Δ and σ respectively. See figure 3.1.

This potential can fulfill the dS-conjecture in a wide inflationary region. It will be helpful to define new fields $(\delta r, \theta, z)$ centered on the track. These relate to (x, y, z) by

$$\begin{aligned} x &= A \cos(z/f) + \delta r \cos \theta \\ y &= A \sin(z/f) + \delta r \sin \theta . \\ z &= z \end{aligned} \quad (3.2)$$

The new field space metric becomes

$$\mathcal{G}_{IJ} = \begin{pmatrix} 1 & 0 & -\frac{A}{f} \sin(z/f - \theta) \\ 0 & \delta r^2 & \frac{A}{f} \delta r \cos(z/f - \theta) \\ -\frac{A}{f} \sin(z/f - \theta) & \frac{A}{f} \delta r \cos(z/f - \theta) & 1 + A^2/f^2 \end{pmatrix} \quad (3.3)$$

and the potential takes the simpler form $V = \Lambda^4 \left(e^{z/R} + \Delta \left(1 - \exp \left[-\frac{\delta r^2}{2\sigma^2} \right] \right) \right)$. In these coordinates ϵ_V takes the form

$$\epsilon_V = \frac{\Delta^2 \delta r^2 R^2 + \sigma^4 e^{\frac{\delta r^2}{\sigma^2} + \frac{2z}{R}}}{2R^2 \sigma^4 \left(\Delta - e^{\frac{\delta r^2}{2\sigma^2}} (\Delta + e^{z/R}) \right)^2}. \quad (3.4)$$

For later convenience we also define the Cartesian offsets from the center of the track $\delta x = x - A \cos(z/f)$ and $\delta y = y - A \sin(z/f)$, such that $\delta r^2 = \delta x^2 + \delta y^2$.

This potential can satisfy the refined dS conjecture in a wide inflationary region. At constant z and far away from the track or along its center ($\delta r \rightarrow 0, \infty$), $\epsilon_V \rightarrow 1/(2R^2)$, so we can fulfill the conjecture in this limit with the choice of a small enough R . The walls of the track are always steeper than its center, so the entire track fulfills the conjecture if the center does. However, away from the track in the $z \rightarrow -\infty$ limit, $\epsilon_V \rightarrow 0$, so this region of the potential does not fulfill the conjecture. Because this region is distant from the inflationary region ($\epsilon_V = 10^{-3}$ at $\Delta\phi \sim 7.3M_{\text{Pl}}$ from the start of inflation using the parameters in Figure 3.3) and the swampland distance conjecture tells us that we should not trust effective field theories in asymptotic field space anyway, we do not consider its presence to diminish our argument.

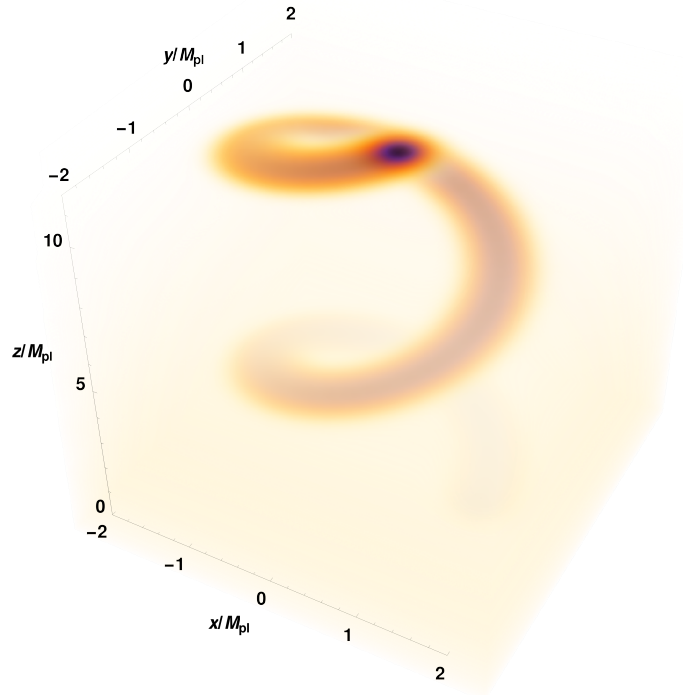


Figure 3.1: The helix-path potential (3.1). The potential is plotted so that cloud density increases as V decreases. Note that the center of the helical track is always a constant Δ lower than its surroundings, while the decrease in the $e^{z/R}$ term appears as an increasing cloudiness in the volume around the helix towards the bottom of the plot, partially hiding it from view. We encourage readers to view this plot in color. Parameters chosen for this plot were illustrative and not in the regime of inflationary interest.

3.1 Background dynamics

The background equations of motion are

$$\begin{aligned}
H^2 &= \frac{V}{3 - \epsilon_H} \\
\delta r'' + (3 - \epsilon_H)\delta r' - \delta r \theta'^2 + \frac{A}{f^2} \cos(z/f - \theta) z'^2 + \\
&+ \frac{\Lambda^4}{H^2} \left(\frac{\Delta \delta r}{\sigma^2} e^{-\delta r^2/(2\sigma^2)} \left(1 + \frac{A^2}{f^2} - \frac{A^2}{f^2} \cos^2(z/f - \theta) \right) + \frac{A e^{z/R}}{fR} \sin(z/f - \theta) \right) = 0 \\
\theta'' + (3 - \epsilon_H)\theta' + 2 \frac{\delta r' \theta'}{\delta r} - \frac{A}{f^2 \delta r} \sin(2z/f - 2\theta) z'^2 + \\
&+ \frac{\Lambda^4 A}{2f^2 H^2} \left(-\frac{A \Delta e^{-\delta r^2/(2\sigma^2)} \sin(2z/f - 2\theta)}{\sigma^2} - \frac{2f e^{z/R} \cos(z/f - \theta)}{R \delta r} \right) = 0 \\
z'' + (3 - \epsilon_H)z' + \frac{\Lambda^4}{H^2} \left(\frac{A \Delta \delta r}{f \sigma^2} e^{-\delta r^2/(2\sigma^2)} \sin(z/f - \theta) + \frac{1}{R} e^{z/R} \right) = 0
\end{aligned} \tag{3.5}$$

where primes denote e-fold derivatives $\partial_t \equiv H \partial_N$. Note that the background evolution depends only on the combination Λ^4/H^2 , which is independent of Λ . However, the same is not true for the perturbations. We will later exploit this to set the amplitude of the scalar perturbations without affecting the background evolution.

There is a steady-state solution with the fields approximately centered in the helical track, which we give in appendix A. We term this solution “steady-state” because all of its slow-roll parameters are constants in time. It is analytically tractable, and gives high-slope inflation ($\epsilon_V \gg \epsilon_H$) in a wide region of parameter space. Numerically, small perturbations ($\Delta \delta r \lesssim \sigma/4$) around the trajectory converge to the steady-state solution. As we show in the appendix, while classically viable, this solution generates an observationally-excluded tensor power so we will not study it here.

Some perturbations around the steady-state solution only converge to it at late times – we term these “metastable” solutions. As we show in subsection 3.2 below, this model’s Planck-compatible regions of parameter space correspond to this class of solutions. We lack an analytic description of these metastable dynamics³, which we compare to the steady-state dynamics in Figure 3.2. In brief, the metastable solution falls much more slowly in the z direction, with $z'_{\text{metastable}} \sim z'_{\text{steady-state}}/3$ initially. Due to the decreased velocity down the helix, the fields also stay closer to its center, with $\delta x_{\text{metastable}}$ and $\delta y_{\text{metastable}}$ smaller than their steady-state counterparts. We present the slow-roll parameters of one realization of the metastable solution in Figure 3.3. These parameters give $\epsilon_V \sim 0.5$ outside the track, and a turning rate $\omega^2/H^2 \sim 10^4$.

The steady-state solution has a constant ϵ_H as is common to exponential inflation, so inflation does not end. The metastable solution in the regime of interest has $\epsilon_H < \epsilon_{H \text{ steady-state}}$,

³Many of our parameter selections were found with a differential evolution optimizer from the `BlackBoxOptim.jl` package [166], applied to our Julia-language implementation of the transport method [167].

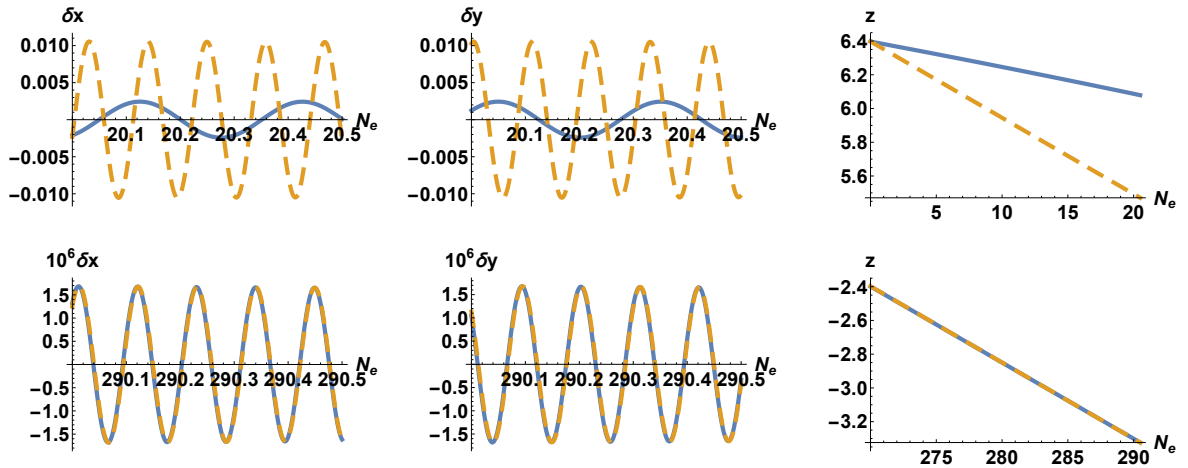


Figure 3.2: A comparison of metastable (blue) and steady-state (dashed, yellow) dynamics in the helix potential (3.1), without the inflation-ending modification (3.6). In the top row, we plot $(\delta x, \delta y, z)$ in units of M_{Pl} at an early time, when the metastable solution has a smaller z' , and smaller orbit around the helix's center in the x, y -plane. In the bottom row, the metastable solution has converged to a steady-state solution (with a different initial z than the metastable solution) by $N_e \simeq 290$.

so it also cannot end inflation. However a small modification to the potential can end inflation without affecting the background behavior during the moment of horizon-crossing, and leave the perturbations invariant. We take the depth of the track to vary along the motion, so that it decreases as

$$\Delta(z) = \Delta_0 \tanh\left(\frac{z - z_{\text{end}}}{f_t}\right) \quad (3.6)$$

where $\Delta(z_0) \approx \Delta_0$, and $\epsilon_H \rightarrow 1$ occurs approximately when $z \rightarrow z_{\text{end}}$.

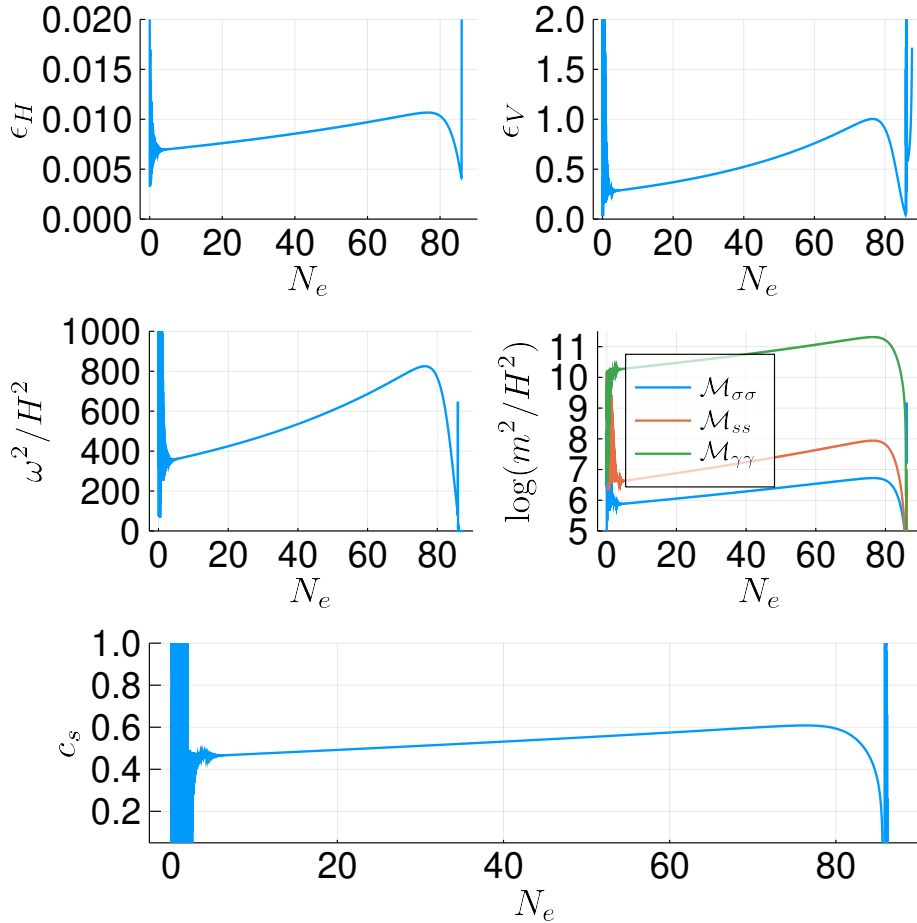


Figure 3.3: Background evolution for the helix potential (3.1), with inflation-ending modification (3.6). Parameter values used were $R = 1.07M_{\text{Pl}}$, $\Delta_0 = 8.44$, $A = 3.47 \times 10^{-3}M_{\text{Pl}}$, $f = 7.85 \times 10^{-4}$, $\sigma = 8.9 \times 10^{-3}M_{\text{Pl}}$, $f_t = 0.1M_{\text{Pl}}$. The initial value of z and z_{end} were chosen to give 87.6 e-folds. The excursion covered is large, but not asymptotically so $\Delta\phi \sim 1.5M_{\text{Pl}}$ ($3.1M_{\text{Pl}}$) in the unmodified (modified) potential. The difference in excursion, compared to the unmodified case, occurs during the last 0.1 e-folds.

3.2 Perturbations

As can be seen in Figure 3.3, the two entropic masses are both larger than the adiabatic mass. With heavy isocurvature masses, multi-field inflationary scenarios with high turning rates produce perturbations similarly to single-field models with a reduced speed of sound c_s . This has been rigorously derived for two-field scenarios in [168–170] and for three-field scenarios in [171]. This effective single-field theory becomes more accurate as the gap between the adiabatic and entropic masses grows. Although in our case the masses are not parametrically separated, we can study the single-field effective theory from integrating them out, knowing that it is subject to $\mathcal{M}_{\sigma\sigma}/\mathcal{M}_{\text{entropic}}$ corrections.

In our notation, the effective speed of sound is

$$\frac{1}{c_s^2} = 1 + \frac{4\omega^2(V_{\gamma\gamma} - |\dot{\gamma}|^2)}{\det M} \quad (3.7)$$

$$M \equiv \begin{pmatrix} V_{ss} - \omega^2 - |\dot{\gamma}|^2 & V_{s\gamma} \\ V_{s\gamma} & V_{\gamma\gamma} - |\dot{\gamma}|^2 \end{pmatrix}$$

where s^I and γ^I are normal and binormal unit vectors to the trajectory as in (2.6). For the fields x, y, z in flat space, $\hat{\gamma} \equiv \hat{\sigma} \times \hat{s}$.

The perturbations of single-field models with reduced speed of sound are well studied [168, 169, 172]. The spectral tilt in such models is

$$n_s - 1 \simeq -2\epsilon_H - \eta_H - \kappa \quad (3.8)$$

where $\kappa \equiv c'_s/c_s$. Similarly the tensor-to-scalar ratio is given by

$$r = 16\epsilon_H c_s \quad (3.9)$$

which is suppressed in the small c_s limit. The equilateral non-gaussianity is inversely proportional to c_s , however, so the sound speed cannot be made arbitrarily small and agree with observations.

$$f_{NL}^{(\text{eq})} = \frac{125}{108} \frac{\epsilon_H}{c_s^2} + \frac{5}{81} \frac{c_s^2}{2} \left(1 - \frac{1}{c_s^2}\right)^2 + \frac{35}{108} \left(1 - \frac{1}{c_s^2}\right) \quad (3.10)$$

In our steady-state solution, $\eta_H \approx \kappa \approx 0$, and $c_s \gtrsim 0.8$. This solution, then, influences n_s only by the effects of ϵ_H , and a large ϵ_H is needed for n_s to be Planck-compatible. Unfortunately, this also raises the expected tensor power, r , observationally excluding this solution. Our metastable solution, however, has a much smaller c_s and cannot be excluded by the same reasoning. η_H and κ , while small, are not negligible. This argument was verified with a full transport method evolution of the perturbations, which is equivalent to tree-level in the in-in formalism (see appendix B for a brief overview of the method). The powerspectra corresponding to the background evolution in figure 3.3 are shown in figure 3.4.

We emphasize these models have low isocurvature ($r_{\text{iso}} \equiv P_{\text{iso}}(k_*, N_{\text{end}})/P_{\zeta}(k_*, N_{\text{end}}) \sim 10^{-4}$) and a featureless adiabatic powerspectrum. The computed values of n_s and r lie within the 2σ Planck ellipse in the n_s - r plane. Tensor modes are speed-of-sound suppressed, with $c_s \sim 0.5$.

We did not perform any numerical analysis of the bispectrum of perturbations, but the effective single-field result can give an estimate. For the horizon-exit value of an $\epsilon_H \sim 0.006$, a sound speed of $0.1 \lesssim c_s$ is consistent with the 1σ value from Planck 2018 [173, 174]. With the speed of sound in figure 3.4 we estimate $f_{NL}^{(\text{eq})} \simeq -18$, well within the 1σ bound.

The EFT results for n_s and r do not agree exactly with their transport-method counterparts: $n_s|_{\text{EFT}} - n_s|_{\text{transport}} \sim 0.005$ and $r|_{\text{EFT}} = 0.0676 \sim 1.87r|_{\text{transport}}$. The EFT is not in its full regime of validity, due to the relatively small mass gap between $\mathcal{M}_{\sigma\sigma}$ and \mathcal{M}_{s_s} . Nonetheless, we expect a full numerical calculation of $f_{NL}^{(\text{eq})}$ to be Planck-compatible, given that we would need almost an effective c_s a factor of 5 lower to reach 1σ tension with the Planck result. It would be interesting to explore the full transport-method evolution and shape of this model's bispectrum. In addition to equilateral non-gaussianity, $c_s \neq 1$

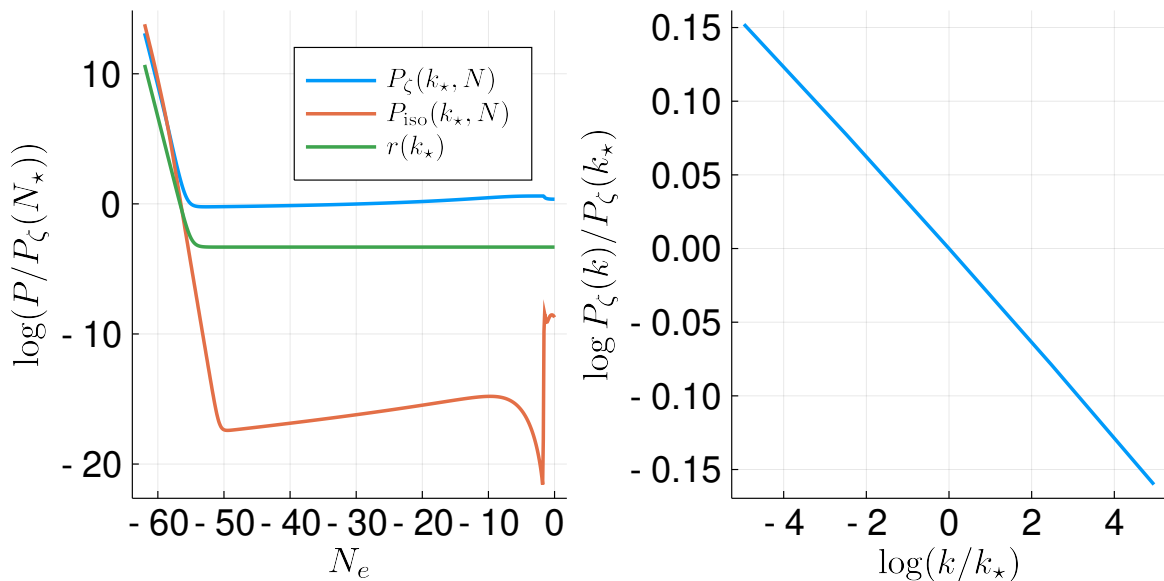


Figure 3.4: Powerspectra of scalar and tensor modes during the background dynamics of Figure 3.3, evolved with the transport method. The plot begins when we impose Bunch-Davies initial conditions for the modes, and ends at the end of inflation. Horizon exit occurs at $N_* = -55$ for the pivot scale $k_* = 0.002 \text{ Mpc}^{-1}$. This simulation has tensor-to-scalar ratio $r = 0.036$ and the spectral index $n_s = 0.9685$. At the end of inflation, isocurvature power is suppressed by a factor of $\sim 10^4$.

trajectories have also been proposed to generically source large non-gaussianities in folded configurations [15, 175].

The model presented here is the first flat field space high-turning rate inflationary solution consistent with the dS-conjecture – it also has Planck-compatible regions of parameter space. The predicted tensor power is relatively high, and within the range of upcoming experiments, e.g. LiteBIRD [176]. Effective reduced speed-of-sound models virtually guarantee either relatively large tensor modes ($r \gtrsim 10^{-3}$) or large equilateral non-gaussianity, and increased bounds on both would tightly constrain this type of track-like construction.

4 Superpotential model

In this section we study, and then modify, an analytically simple model with negative field-space curvature studied by Chen et al. [177] in the context of primordial non-gaussianities. This is a particular case of a larger family of potentials analyzed in [59, 162] that is conducive to analytical results. We begin by highlighting the model’s desirable classical behavior: it can achieve a sufficiently high number of e-folds of inflation with distinctly non-geodesic motion, while globally satisfying the refined de Sitter conjecture (1.2). We then discuss the challenges of making the quantum fluctuations’ phenomenology sound. The single-field EFT used in section 3 breaks down, so analysis of the perturbations must be entirely two-field. When combined with the negative field-space curvature, a high rate of turning is known to yield an exponential growth of the perturbations before horizon exit. This is not fatal, but bounds the turning rate from above to prevent the scale of inflation from dipping below the

nucleosynthesis scale. This section shows that it is possible to construct a model that satisfies all these constraints.

The model has two fields, $\phi^I = \{X, Y\}$, with a hyperbolic metric:

$$\mathcal{G}_{IJ} = \begin{pmatrix} e^{2Y/R_0} & 0 \\ 0 & 1 \end{pmatrix} \quad (4.1)$$

with non-vanishing Christoffel symbols and Riemann tensor components

$$\begin{aligned} \Gamma_{XY}^X &= \Gamma_{YX}^X = \frac{1}{R_0} & R_{XXY}^Y &= -R_{XYX}^Y = \frac{1}{R_0^2} e^{2Y/R_0} \\ \Gamma_{XX}^Y &= -\frac{1}{R_0} e^{2Y/R_0} & R_{YYX}^X &= -R_{YXY}^X = \frac{1}{R_0^2}. \end{aligned} \quad (4.2)$$

The potential is built from a ‘‘superpotential,’’ $W = W(X)$:

$$V(X, Y) = 3W^2 - 2\mathcal{G}^{IJ}W_{,I}W_{,J}. \quad (4.3)$$

Note that due to the minus sign and the dependence on real-valued fields, W is not a true superpotential; we use the term simply for convenience. This form of the potential⁴ can be realized in two ways: by demanding that inflation occurs along an isometry direction of the metric [59], or by enforcing $\dot{Y} = 0$ and a potential of the form $V(X, Y) = h(X) + f(X)g(Y)$; see Appendix C for a derivation. The dynamics are given by:

$$\dot{\phi}^I = -2\mathcal{G}^{IJ}W_{,J} = \left(-2e^{-2Y/R_0}W_{,X}, 0 \right) \quad (4.4)$$

$$H = W \quad (4.5)$$

$$\omega^I = \left(0, \frac{2}{R_0} e^{-Y/R_0} W_{,X} \right) \quad (4.6)$$

$$\epsilon_H = \frac{R_0^2}{2} \frac{\omega^2}{H^2}. \quad (4.7)$$

In consideration of the de Sitter conjecture, we can constrain the geometric scale R_0 by imposing high-turning, slow-roll inflation independent of the form of the superpotential: choosing $\omega/H \gtrsim 10^1$ and $\epsilon_H \lesssim 10^{-2}$ fixes $R_0 \lesssim 10^{-2}$.

An exponential superpotential,

$$W = Ae^{X/R_1}, \quad (4.8)$$

can easily meet $\epsilon_H \ll 1$, $\epsilon_V \gtrsim 1$, and $\omega/H \gg 1$ along the trajectory for all time. We find the following analytic results:

$$Y(N) = Y_0, \quad X(N) \equiv X_N = X_0 - \frac{2}{R_1} e^{-2Y_0/R_0} N \quad (4.9)$$

$$N(t) = \frac{R_1}{2} e^{2Y_0/R_0} \log \left[\frac{2A}{R_1^2} e^{X_0/R_1 + 2Y_0/R_1} t + 1 \right] \quad (4.10)$$

$$\frac{\omega}{H} = \frac{2}{R_0 R_1} e^{-Y_0/R_0} \quad (4.11)$$

$$\epsilon_H = \frac{2}{R_1^2} e^{-2Y_0/R_0} \quad (4.12)$$

$$\epsilon_V = \frac{2}{R_1^2} e^{-2Y/R_0} + \frac{8}{R_0^2} \frac{1}{(3R_1^2 e^{2Y/R_0} - 2)^2}. \quad (4.13)$$

⁴Note that models with a similar field space metric and different potentials have been presented in [13, 178]

Here, N is the number of e-folds elapsed since the start of inflation, and t is cosmic time. We note that the superpotential scale R_1 cannot be chosen independently of Y_0 while maintaining slow-roll inflation. Using the above constraint on R_0 , we find $e^{-Y_0/R_0}/R_1 = \sqrt{\epsilon_H}/2 \lesssim 10^{-1}$. Hence, there exists a one-dimensional family of values for R_1 and Y_0 with the desired inflationary behavior. We further emphasize that ϵ_V parametrizes potential gradients throughout the entire field space, whereas the dynamical expressions above pertain to a particular inflationary trajectory.

We observe that the inflationary trajectory (4.9) proceeds in the negative X direction at a fixed value of Y . The “turning” of this path can be seen by comparing against geodesics of this field space, which take the form:

$$\tilde{Y}(X) = R_0 \log \left[\frac{R_0}{\sqrt{C - X} \sqrt{K - C + X}} \right]. \quad (4.14)$$

A derivation is presented in Appendix D. The constants K and C may be chosen such that the geodesic passes through any two points (X_1, Y_1) and (X_2, Y_2) such that $X_1 \neq X_2$; their values are given in (D.11) and (D.12). Evidently, the trajectory (4.9) is strongly non-geodesic, with rapid turning for appropriately chosen parameters R_0 , R_1 , and Y_0 .

An important feature of this class of trajectories is that field excursions are easily made sub-Planckian due to the small value of R_0 . This ensures that the effective field theory with scalar potential (4.3) does not break down over the course of inflation [18, 19]. The excursion is defined as the geodesic distance between two points (X_i, Y_i) and (X_f, Y_f) and is given by (D.15). We consider a trajectory from the initial point $(X_i, Y_i) = (X_0, Y_0)$ up until the point corresponding to N e-folds of inflation $(X_f, Y_f) = (X_N, Y_0)$. Choosing a geodesic that passes through these points, the expressions for K and C simplify:

$$K = \sqrt{(X_N - X_0)^2 + 4Q} \quad (4.15)$$

$$C = \frac{X_N + X_0 + K}{2}, \quad (4.16)$$

where $Q = R_0^2 e^{-2Y_0/R_0}$. The geodesic distance (D.15) reduces to

$$S = \frac{R_0}{2} \log \left[\left(\frac{X_0 - X_N + K}{X_0 - X_N - K} \right)^2 \right]. \quad (4.17)$$

The small geometric scale R_0 , required to have high-turning inflation, strongly suppresses the distance for many possible values of X_0 and X_N , which ensures that the potential is valid throughout inflation. A sample trajectory with rapid turning and sub-Planckian field excursion is displayed in Figure (4.1) with the corresponding geodesic connecting X_0 and X_N .

We note that ϵ_V vanishes for $Y \gg R_0$. Although this conflicts with the gradient swampland conjecture, we find that the refined de Sitter conjecture [19] still holds. In particular, this model satisfies the right half of (1.2): η_V is globally negative. Since the superpotential is chosen to be an exponential, η_V is independent of X for this model. Figure (4.2) displays η_V as a function of Y , with asymptotic values that are $\mathcal{O}(-1)$. Therefore, this potential indeed satisfies the refined de Sitter conjecture globally, in spite of ϵ_V vanishing for Y sufficiently large.

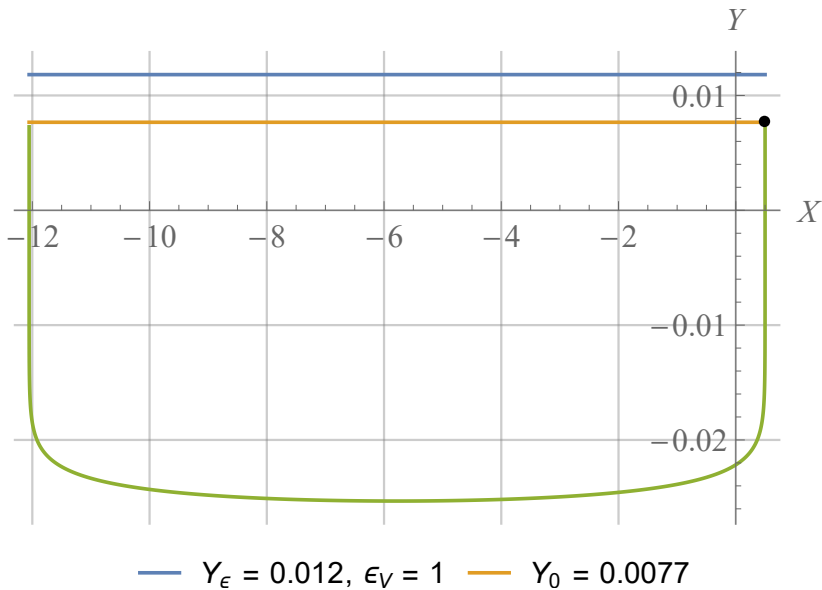


Figure 4.1: A trajectory of the form (4.9) with $N = 300$ e-folds of inflation with $X_0 = 0.5$, $X_N = -12.05$, $Y_0 = 0.0077$, $R_0 = 0.0034$, and $R_1 = 0.5$. The geodesic connecting (X_0, Y_0) to (X_N, Y_0) extends below the trajectory and yields a field excursion of $0.071 M_{\text{Pl}}$. The line at $Y_\epsilon = 0.012$ corresponding to $\epsilon_V = 1$ is highlighted as well, with $\epsilon_V > 1$ everywhere below this line.

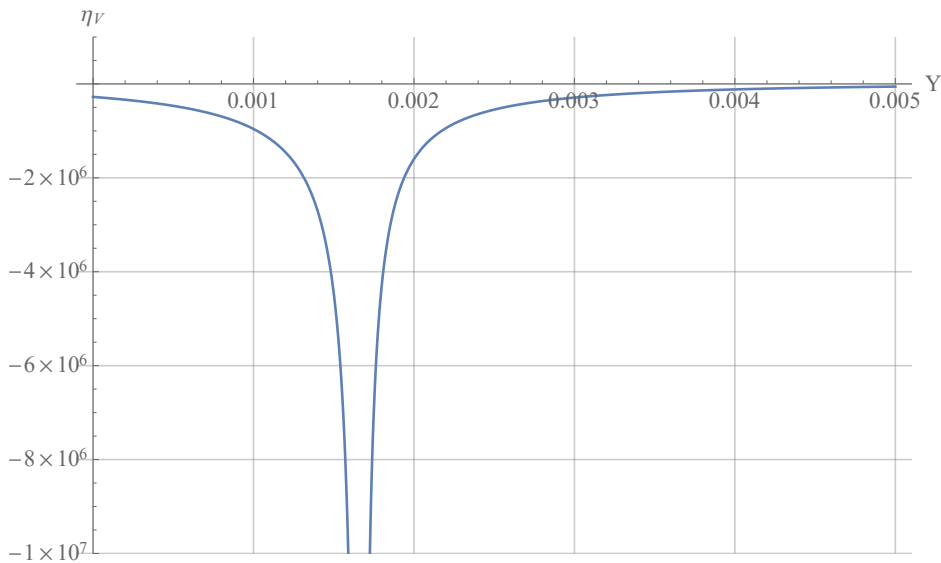


Figure 4.2: The minimum eigenvalue of the covariant Hessian matrix for $R_0 = 0.0034$ and $R_1 = 0.5$. This quantity is independent of X . The asymptotic behavior arises from the potential V vanishing at $Y = 0.00167$ and becoming negative below this value. For large positive and negative Y , η_V asymptotes to approximately -3 and -20 respectively, thus satisfying the refined de Sitter swampland conjecture.

Furthermore, we observe that there are values of Y for which neither conjecture regarding the potential need be satisfied, namely those at which the potential becomes negative:

$$Y < \frac{R_0}{2} \log \left[\frac{2}{3(R_1)^2} \right]. \quad (4.18)$$

The classical solution does not yield inflation in this region, since this corresponds to $\epsilon_H > 3$ along the trajectory. Hence, initial conditions must be chosen such that this region is avoided.

The primary drawback to this model lies in η_H being identically 0, so inflation does not end⁵. In order to terminate inflation, we seek an alternate superpotential such that ϵ_H crosses unity from below. In particular, we choose a function that preserves the exponential behavior at asymptotic values of X . Consider:

$$W(X) = Ae^{X/R_1} \left[\tanh \left(\frac{X}{R_2} \right) + 1 \right]. \quad (4.19)$$

This modification preserves the positivity of the superpotential, and hence the Hubble parameter. From (4.4), the equations of motion are:

$$\dot{X} = -2Ae^{-2Y_0/R_0} e^{X/R_1} \left[\frac{\tanh(X/R_2)}{R_1} + \frac{\text{sech}^2(X/R_2)}{R_2} \right], \quad \dot{Y} = 0. \quad (4.20)$$

The slow-roll parameter for this model is of the form

$$\epsilon_H = \frac{2e^{-\frac{2Y}{R_0}} \left[2R_1 + R_2 \left(e^{\frac{2X}{R_2}} + 1 \right) \right]^2}{R_1^2 R_2^2 \left(e^{\frac{2X}{R_2}} + 1 \right)^2}, \quad (4.21)$$

which increases monotonically as X decreases from its initial value. This ensures that inflation terminates after a finite number of e-folds.

Unlike (4.13), the value of ϵ_V for this superpotential depends on both fields X and Y , although it still does not globally remain $\mathcal{O}(1)$ or larger. However, parameters of the model can be chosen such that η_V is bounded from above by $\mathcal{O}(-1)$ values everywhere, except in a one-dimensional region near $X = 0$ where the \tanh factor dominates; see Figure (4.3). Fortunately, the parameter space allows for $\epsilon_V \gtrsim 1$ in this region, so long as the turning rate on the trajectory is sufficiently large. Therefore, the refined de Sitter conjecture remains satisfied.

The quantum perturbations in this model are well studied, since it is a subclass of orbital inflation [59] and of the broader category of models studied in [162]. A notable feature of this class of one-field superpotentials is the simplicity of the first order equations of motion, which allows for the mass-squared matrix (2.4) to be easily computed. The adiabatic component is of the form:

$$\mathcal{M}_{\sigma\sigma} = \omega^2 + 6H^2\epsilon_H - \frac{3}{2}H^2\eta_H + \frac{5}{2}H^2\epsilon_H\eta_H - \frac{1}{4}H^2\eta_H^2 - 2H^2\epsilon_H^2 - \frac{1}{2}H\dot{\eta}_H. \quad (4.22)$$

Note that for high-turning inflation, $\mathcal{M}_{\sigma\sigma} \simeq \omega^2 + \mathcal{O}(\epsilon_H, \eta_H)$. The entropic component has the form

$$\mathcal{M}_{ss} = -\frac{12}{R_0^2} e^{-2Y_0/R_0} W_X^2 = -3\omega^2. \quad (4.23)$$

⁵In the sense of [41], background motion with constant slow-roll parameters can be seen as the critical point of a dynamical system.

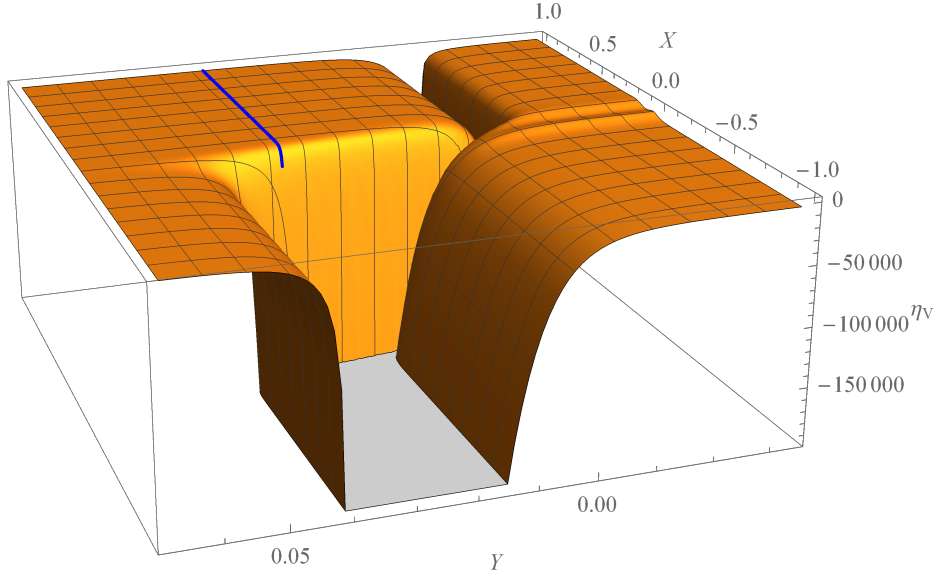


Figure 4.3: The minimum eigenvalue of the covariant Hessian matrix in the vicinity of the trajectory for (4.19) with $R_0 = 0.011$, $R_1 = 1.82$, and $R_2 = 0.05$. For large positive Y , η_V asymptotes to -3.00 . For large negative Y and large positive X , η_V asymptotes to -1.51 , becoming even more negative for large negative values of X . For negative values of Y in the vicinity of $X = 0.15$, η_V has a local maximum that is positive, but $\epsilon_V > 1$ in this region. Hence, the refined de Sitter swampland conjecture is satisfied. The value of η_V along the trajectory is highlighted in blue. The trajectory is chosen to begin at $X_0 = 1$ along a constant value of $Y_0 = 0.034$. The turning rate and slow-roll parameter are approximately constant at $\omega/H = 4.84$ and $\epsilon_H = 0.0015$, respectively, until the very end of inflation, when ϵ_H quickly rises and crosses unity at $X_N = 0.016$. This trajectory yields $N = 328$ e-folds of inflation and a field excursion of $0.17 M_{\text{Pl}}$.

Hence on subhorizon scales, the effective entropic mass $\mu_{s,\text{sub}}^2 = \mathcal{M}_{ss} - \omega^2$ is negative and large in magnitude, due to the nontrivial turning rate^{6,7}. From (2.11) and (2.5), we see that this sources an exponential growth of both the adiabatic and entropic power for modes with $k^2/(aH)^2 < 4\omega^2/H^2$. This is a manifestation of the tachyonic instability of modes with a large and negative $\mu_{s,\text{sub}}^2/H^2$ discussed in [49].

On superhorizon scales our model has an exactly massless entropic perturbation, as shown in [59] and [162]. This is a consequence of a flat direction in the effective potential, whose gradient is

$$V_{\text{eff}}^\alpha = V^\alpha + 2\epsilon_H H^2 \Gamma_{\sigma\sigma}^\alpha, \quad (4.24)$$

where α indexes non-adiabatic directions. In this case, V_{eff}^y is identically zero.

After horizon exit, entropic perturbations will freeze, as seen from (2.11). As long as $\omega/H \gtrsim 1$, the entropic modes will feed the growth of the adiabatic modes causing them

⁶This precise value of the entropic mass violates the criteria of validity for the usual single-field EFT, see appendix A of [179]. The speed of sound ($c_s^{-2} = 1 + 4\omega^2/\mu_{s,\text{sub}}^2$) diverges. For this reason, our analysis in this section is strictly two-field.

⁷These masses' dependence on ω agrees with the rapid-turn inflationary attractor [43].

to grow linearly with time. This feature reduces the ratio of the entropic power over the adiabatic power as inflation continues and ω/H remains large.

We now estimate the degree of exponential growth, x , of the power spectrum:

$$P_{\mathcal{R}} = \frac{H_{\star}^2}{8\pi^2\epsilon_{H\star}} e^{2x}. \quad (4.25)$$

Following the notation of [43, 161], we express the entropic component of the mass-squared matrix (2.4) as:

$$\mathcal{M}_{ss} \equiv \xi\omega^2. \quad (4.26)$$

From (4.23), we see that one-field superpotential models have $\xi = -3$. The equations of motion (2.5) and (2.8) can then be recast in terms of the curvature scalar \mathcal{R}_c as:⁸

$$\ddot{\mathcal{R}}_c + 3(H + \eta_H)\dot{\mathcal{R}}_c + \frac{k^2}{a^2}\mathcal{R}_c = \frac{2\omega}{\sqrt{2\epsilon_H}} \left[\dot{Q}_s + (3 - \epsilon_H)HQ_s \right] \quad (4.27)$$

$$\ddot{Q}_s + 3H\dot{Q}_s + \left[\frac{k^2}{a^2} + (\xi - 1)\omega^2 \right] Q_s = -2\omega\sqrt{2\epsilon_H}\dot{\mathcal{R}}_c. \quad (4.28)$$

In order to find the growth parameter x , we employ the WKB method as used in [161], without dropping the Hubble friction terms in (4.27) and (4.28). We note that the slow-roll suppressed terms in (4.27) can be safely neglected in this computation. Anticipating an exponential amplification of both modes, we assume a solution of the form:

$$\mathcal{R}_c = \mathcal{R}_c^{(0)} e^{\lambda t}, \quad Q_s = Q_s^{(0)} e^{\lambda t}. \quad (4.29)$$

Inserting this ansatz into (4.27) and (4.28), enforcing $\lambda > 0$, and setting $\xi = -3$ for our model, we find:

$$\tilde{\lambda} \equiv \lambda/H = \frac{1}{2} \left[-3 + \sqrt{9 - 4(\kappa^2 - 2\kappa\omega/H)} \right], \quad (4.30)$$

where $\kappa \equiv \frac{k}{aH}$. Note that a positive λ requires $\kappa < 2\omega/H$; since κ decays with the number of e-folds elapsed, the exponential growth begins at $N = -\log(2\omega/H)$ before horizon crossing. The adiabatic mode then grows as:

$$\mathcal{R}_c \sim \exp \left[\int_{-\log(2\omega/H)}^N |\tilde{\lambda}| dN' \right]. \quad (4.31)$$

As shown in [59], we can solve (4.27) and (4.28) on superhorizon scales to find:

$$Q_s = \frac{H_{\star}}{2\pi}, \quad |\mathcal{R}_c|_{\text{super}}^2 = \frac{N_{\star}^2 \omega_{\star}^2}{2\pi^2 \epsilon_{H\star}} \quad (4.32)$$

The total adiabatic power including sub- and superhorizon contributions is then:

$$P_{\mathcal{R}} = \frac{H_{\star}^2}{8\pi^2\epsilon_{H\star}} \exp \left[2 \int_{-\log(2\omega/H)}^{\infty} |\tilde{\lambda}| dN' \right] \left(1 + \frac{4N_{\star}^2 \omega_{\star}^2}{H_{\star}^2} \right). \quad (4.33)$$

⁸Rewriting the equations in this form also allows us to check the stability of the background trajectory by computing the Lyapunov exponents as in [43, 57]. To lowest order in slow-roll parameters, the exponents are $0, 0, -3H, -3H$. All are zero or negative, ensuring stability.

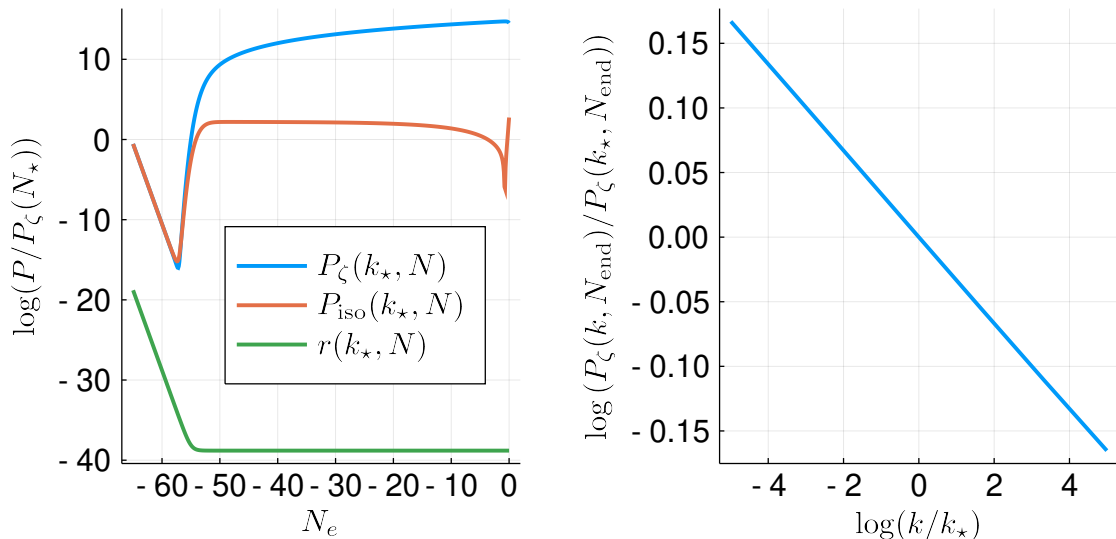


Figure 4.4: Perturbative powerspectra for the pivot-scale mode in the superpotential model, with Bunch-Davies initial conditions numerically imposed well before any subhorizon growth at 10 e-folds before horizon exit. The scalar powerspectra give $n_s = 0.966$ and $r_{\text{iso}} \sim 10^{-6}$. Tensor modes are exponentially small, with both the sub- and superhorizon growth of the adiabatic mode giving $r \sim 10^{-17}$ by the end of inflation. We measure a growth parameter $x = 15.371$, in good agreement with (4.34).

Comparing this against (4.25), we solve for the effective growth parameter at the end of inflation:

$$x = \int_{-\log(2\omega/H)}^{\infty} |\tilde{\lambda}| dN' + \frac{1}{2} \log \left(1 + \frac{4N_*^2 \omega_*^2}{H_*^2} \right). \quad (4.34)$$

Solving the integral numerically, this yields $x = 14.962$ for $\omega_*/H_* \sim 4.84$. Fitting the transport-method adiabatic power spectrum in Figure 4.4 yields $x = 15.371$. We observe that this agrees remarkably with the WKB calculation so long as the superhorizon contribution to the adiabatic power is also included. Including the Hubble friction terms in (4.27) was also important – neglecting them predicts $x \sim 21$, a much higher growth. Comparing this against (4.25) and taking $\epsilon_H = 0.0015$ from Figure (4.3), we find a value for the Hubble parameter:

$$H_* \sim 10^{-12} M_{\text{Pl}} \sim 10^6 \text{ GeV}. \quad (4.35)$$

Thus, the parameter space permits a mass scale of inflation compatible with nucleosynthesis bounds, $H_{\text{min}} \approx 4 \text{ MeV}$, so long as the turning rate is not excessively large. Saturating the nucleosynthesis bound requires:

$$x = \frac{1}{2} \log \left(\frac{8\pi^2 \epsilon_{H_*}}{H_{\text{min}}^2} \right) \simeq 46 + \log \left(\frac{\epsilon_{H_*}}{0.0015} \right)^{1/2}. \quad (4.36)$$

For $\epsilon_{H_*} = 0.0015$, this sets an upper bound on the turning rate, $\omega \lesssim 15$.

In [49], the authors use the single-field EFT to estimate the growth of flattened non-gaussianities as a function of the growth of the power spectrum for models with an imaginary

speed of sound. We are unable to use their result to reliably compute $f_{\text{NL}}^{\text{flat}}$, due to the invalidity of the EFT for our model.

In summary, superpotentials readily admit classical trajectories with $\epsilon_H \ll 1$, and either $\eta_V \lesssim -1$ or $\epsilon_V \gtrsim 1$ in all regions. The analysis of quantum perturbations shows that the entropic mode effective mass-squared of subhorizon modes, $\mu_{s,\text{sub}}^2 = \mathcal{M}_{ss} - \omega^2$, is large and negative, giving rise to an exponential growth of the perturbations in the subhorizon regime. In order to achieve a scale of inflation compatible with nucleosynthesis, the turning rate must be bounded from above. We emphasize that the parameter space admits trajectories with a desirable turning rate and phenomenology, while satisfying the refined de Sitter conjecture globally.

5 Conclusions

In this work we present two families of multi-field potentials with a high turning rate that support inflation while satisfying the de Sitter and the distance swampland conjectures. One family has a flat field space metric while the other's is negatively curved. We analyze perturbations around the classical solutions and check their predictions against the current CMB experimental bounds.

The flat field space model has three fields and a helix-like potential and has observationally consistent phenomenology. The predicted tensor power is relatively high, and within the range of upcoming experiments, e.g. LiteBIRD. Effectively, this model can be reduced to a single field model with reduced speed of sound. All such models virtually guarantee large tensor to scalar ratio or large equilateral non-gaussianity. This potential does not globally satisfy the refined de Sitter conjectures (1.2), but it does satisfy them around the inflationary trajectory in a region of at least $\mathcal{O}(M_{\text{Pl}})$. We do not know of any UV-complete theory that will produce this type of potential.

In the second part of the paper we analyze a negatively curved field-space metric and a family of orbital-inflation potentials. These are two-field models with a light adiabatic perturbation. The effective entropic mass is large and negative on subhorizon scales and massless on superhorizon scales. As a result, the subhorizon entropic modes source an exponential growth of the adiabatic perturbation. This bounds the turning rate from above in order to keep the mass scale of inflation compatible with nucleosynthesis bounds. The entropic perturbations freeze after horizon crossing while the adiabatic perturbation grows linearly with time. Tensor modes are exponentially suppressed in this model. In addition to terminating after a sufficient number of e-folds, the trajectory's field excursion is easily made sub-Planckian. Furthermore, the potential always has either $\epsilon_V > 1$ or $\eta_V < -1$, thus globally satisfying the refined de Sitter swampland conjecture. This constitutes a previously unexamined model that satisfies the conjectures while achieving prolonged, finite, and phenomenologically viable inflation.

6 Acknowledgements

It is a pleasure to thank Jacques Distler for suggesting helix-like potentials as possible realizations of high-slope inflation and Irene Valenzuela for interesting discussions. We would also like to thank Gonzalo Palma for reviewing an earlier draft of this manuscript and Ana Achúcarro, P. Christodoulidis and D. Roest for comments on the first version of the paper.

This work was supported by the U.S. National Science Foundation under Grants PHY-1521186 and PHY-1620610. This work was initiated at Aspen Center for Physics, which is supported by U.S. National Science Foundation grant PHY-1607611.

A Steady-state solution to helical potential

We look for a solution to the equations of motion (3.5) with

$$\begin{aligned} z' &= -\frac{1}{R} \frac{1}{1 + \frac{A^2}{f^2}} \\ \theta &= z/f + c \\ \delta r &= b e^{z/R} \end{aligned} \tag{A.1}$$

where b, c are constants. Near the center of the track, b is small and we neglect $\mathcal{O}(b^2)$, or $\mathcal{O}(b)$ compared to constant terms in the equations of motion. In addition we neglect the small z -dependence in b and c , since it is $\mathcal{O}(A^2 f^2)$ and we are interested in regime with A and f both small. Our solution ansatz solves the equations of motion when

$$b = \frac{Af\sigma^2 \csc(c)}{(A^2 + f^2)R\Delta} \tag{A.2}$$

$$\tan c = \frac{6R^2(A^2 + f^2) - f^2}{2fR} \tag{A.3}$$

Numerically this solution is stable in a narrow basin of attraction. Small perturbations around this solution $\delta r = b e^{z/R} + \delta\delta r$ are stable when the initial perturbation $\delta\delta r(t_0) \lesssim \sigma/4$. With larger perturbations, either the fields exit the track, or the metastable solution of Figures 3.2 and 3.3 is possible. The metastable solution does eventually converge to this steady-state solution; the metastable phase in Figure 3.2 lasted ~ 250 e-folds before doing so. However in Figure 3.3, we ended inflation during the metastable phase.

The interesting slow-roll parameters are all constants in the steady state:

$$\begin{aligned} \epsilon_H &= M_{\text{Pl}}^2 \frac{1}{2R^2} \frac{1}{1 + A^2/f^2} \\ \epsilon_V &= M_{\text{Pl}}^2 \frac{f^2}{2(A^2 + f^2)^2} \left(\frac{A^2 + f^2}{R^2} + \frac{4A^2 f^2}{(f^2 - 6(A^2 + f^2)R^2)^2} \right) \\ 1 + \frac{\omega^2}{9H^2} &= \epsilon_V/\epsilon_H = 1 + \frac{4A^2 f^2 R^2}{(A^2 + f^2)(f^2 - 6(A^2 + f^2)R^2)^2}. \end{aligned} \tag{A.4}$$

This solution matches our numerics well, see figure A.1.

This solution has high-slope inflation ($\epsilon_V \gg \epsilon_H$) in a large region of parameter space, provided we make A and f both small. The global properties of the potential remain identical to the discussion in section 3. In short, the potential satisfies the refined dS conjecture locally and regions that violate the conjecture are asymptotically far, where the distance conjecture guarantees the effective field theory is invalid anyway.

In this solution, the slow-roll parameters are constant and inflation cannot end. For the simulations in this appendix, we terminated inflation manually once it had become apparent that the perturbations had frozen on superhorizon scales, and were relatively insensitive to

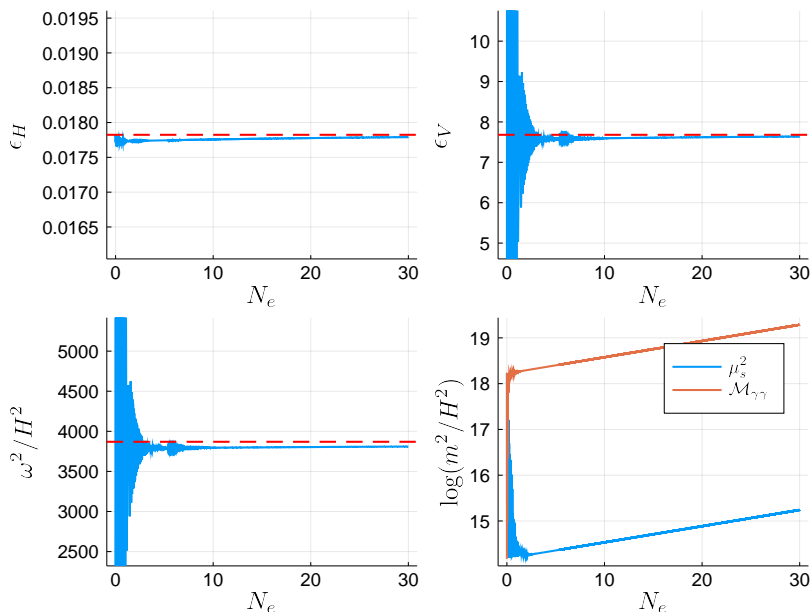


Figure A.1: Slow-roll parameters during the numerical evolution of our helical track potential. The numerical slow-roll parameters are the blue solid lines, and our corresponding steady-state solutions (A.4) are red dotted lines. The deviations from the steady state solution decay proportional to $e^{z/R}$. Initial conditions were chosen slightly off (A.1), which give rise to oscillations as the solution settles into the steady state within a few e-folds. The potential parameters used were $A = 3 \times 10^{-3} M_{\text{Pl}}$, $f = 4 \times 10^{-4} M_{\text{Pl}}$, $\Delta = 2.0$, $R = 0.7 M_{\text{Pl}}$, $\sigma = 10^{-3} M_{\text{Pl}}$. The field-space excursion in this simulation was $\sim 0.7 M_{\text{Pl}}$ over 30 e-folds.

the end of inflation. In our more careful analysis of section 3, our simulations were terminated by inflation ending due to a modification of the potential.

Similarly to the metastable solution in figure 3.3, in figure A.1 the steady-state solution has both entropic masses large during the entire inflationary trajectory, so we expect an effective single-field description to be approximately valid.

In the steady state, taking the limit $b \rightarrow 0$, the speed of sound is

$$c_s = \frac{C + (2A^4 + 2A^2 f^2 (2 - 3R^2) + 3f^4 (1 - 2R^2)) e^{z/R}}{C + (2A^4 + 2A^2 f^2 (9R^2 + 2) + f^4 (18R^2 - 1)) e^{z/R}}, \quad (\text{A.5})$$

$$C \equiv \frac{2\Delta\Lambda^4 R^2 (A^2 + f^2)^4 - 2f^4 \sigma^2 (A^2 + f^2)}{A^2 f^2 \Lambda^4 \sigma^2}$$

The speed of sound can substantially differ from 1 when C is subdominant to the $e^{z/R}$ terms. In the high z/R limit, c_s is minimized by a small ratio of A/f . This expression qualitatively agrees with our numerical calculations of (3.7). For the simulation in figure A.1, $c_s \simeq 1$, but it can be slightly lower⁹.

The spectra tilt in reduced speed-of-sound models is given in (3.8), which we restate here for clarity:

$$n_s - 1 \simeq -2\epsilon_H - \eta_H - \kappa \quad (\text{A.6})$$

⁹Parameters which provide $c_s \sim 0.8$, $n_s \sim 0.96$ are $z_0 = 1.0 M_{\text{Pl}}$, $R = 0.7 M_{\text{Pl}}$, $\Delta = 1.0$, $A = 6 \times 10^{-4} M_{\text{Pl}}$, $f = 8 \times 10^{-5} M_{\text{Pl}}$, $\sigma = 1.3 \times 10^{-3} M_{\text{Pl}}$. In the steady state, this solution has $\omega^2/H^2 \sim 10^5$, $\epsilon_V \sim 190$, $\epsilon_H \sim 0.02$.

In the steady state, $\eta_H \approx 0$ and κ is negligibly small except for the short window of time when C and the $e^{z/R}$ term are comparable in size. This region of time was avoided in our simulations. The adiabatic mode, then, influences n_s only by the effects of ϵ_H . Recalling our steady-state expression (A.4), we expect ϵ_H and therefore n_s to be set by the ratio A/f . Fortunately, this is consistent with our high-slope inflation requirement, which only needs A and f both small. If we take $A/f \sim 7$ and $R \sim \sqrt{2}M_{\text{Pl}}$, then we expect $n_s \sim 0.96$. A simulation with Planck-compatible scalar powerspectra is shown in figure A.2.

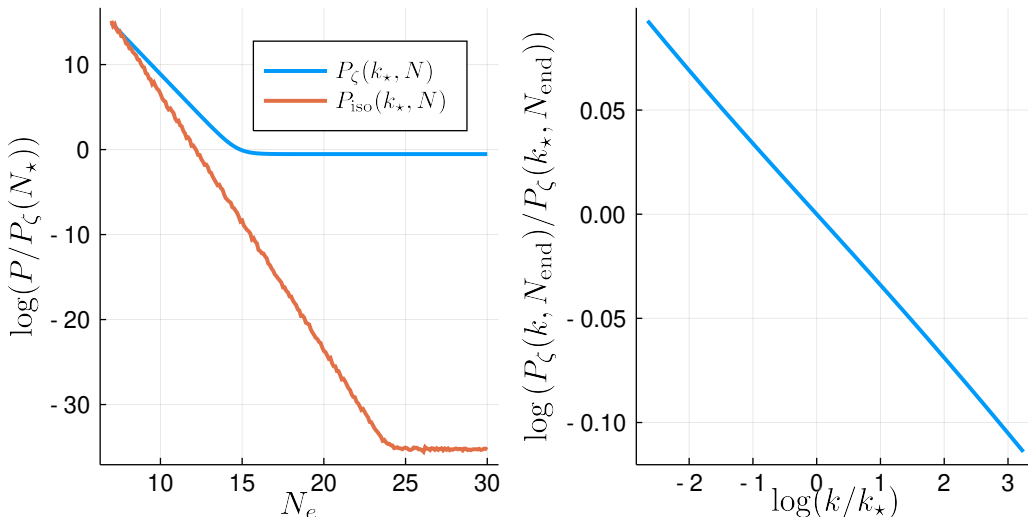


Figure A.2: (Left) The powerspectra for a mode that exited the horizon 15 e-folds after the beginning of inflation. We begin the plot when we numerically imposed Bunch-Davies initial conditions, 8 e-folds before this mode exited the horizon. The adiabatic mode freezes on superhorizon scales, while the isocurvature powerspectra decay until they are numerically indistinguishable from zero. (Right) The adiabatic powerspectrum is smooth and featureless in k , with an $n_s = 0.9653$. Potential parameters match those used in figure A.1.

The steady-state dynamics give low isocurvature ($r_{\text{iso}} \equiv P_{\text{iso}}(k_*, N_{\text{end}})/P_\zeta(k_*, N_{\text{end}}) \sim 0$ within machine precision) and a featureless adiabatic powerspectrum. The scalar powerspectra have frozen out, so we expect these predictions to be largely independent of any late-time modification to the potential to end inflation.

For the steady-state evolution, we did not perform any numerical analysis of the tensor perturbations or bispectrum of scalar perturbations, but applied the single-field EFT to estimate these quantities.

Recalling the single-field EFT results in eqs. (3.8)-(3.10), the ϵ_H in figure A.1 and a $c_s \sim 1$ gives $r \sim 0.32$ and $f_{\text{NL}}^{\text{equ}} \sim 0$.

Because this solution's slow-roll parameters are constants, the only way to achieve a lower r is to lower ϵ_H and therefore raise n_s . This solution's predictions then lie on a line in the n_s - r plane, excluded from the Planck region at $\gtrsim 7\sigma$.

B Transport Method

The transport method [167] is a robust and numerically stable technique for evolving inflationary perturbations. For convenience, we briefly summarize the method here. In this

section lowercase latin indices will run from $0, \dots, 2N_f - 1$, while uppercase latin indices will be consistent with the rest of this paper and run from $1, \dots, N_f$.

In the transport method, rather than evolving the perturbations directly, we evolve their two-point functions. For convenience we define a concatenation of the field and momenta perturbations $X^a \equiv \{Q, \delta\pi\}$, where

$$\delta\pi^I \equiv \partial_N Q^I \quad (\text{B.1})$$

The perturbations' equations of motion (2.3) can be written, to tree level, as

$$\partial_N X^a = u_b^a X^b + \dots \quad (\text{B.2})$$

where

$$u_b^a \equiv \begin{pmatrix} 0 & \delta_B^A \\ -\delta_B^{\bar{A}} \frac{k^2}{a^2 H^2} - \frac{\mathcal{M}_B^{\bar{A}}}{H^2} & \delta_B^{\bar{A}} (\epsilon_H - 3) \end{pmatrix} \quad (\text{B.3})$$

We define the two-point function as

$$\langle X^a(\vec{k}) X^b(\vec{k}') \rangle = \frac{(2\pi)^3}{k^3} \delta(\vec{k} + \vec{k}') \Sigma^{ab}. \quad (\text{B.4})$$

We can evolve the dimensionless two-point function Σ^{ab} in time as

$$\Sigma^{ab}(N) = \Gamma_c^a(N, N_0) \Gamma_d^b(N, N_0) \Sigma^{cd}(N_0) \quad (\text{B.5})$$

$$D_N \Gamma_b^a = u_c^a \Gamma_b^c \quad (\text{B.6})$$

where D_N is a covariant e-fold derivative and $\Gamma_b^a(N, N_0)$ propagates the evolution from a time with known initial conditions N_0 , to a later time N .

When a mode is sufficiently subhorizon, Σ^{ab} will be approximately the dimensionless two-point function of a Bunch-Davies state. For a mode with wavenumber k , this is

$$\Sigma^{ab}|_{\text{BD}} = \begin{pmatrix} \frac{H^2 \mathcal{G}^{IJ}}{2} |k\tau|^2 & -\frac{H^2 \mathcal{G}^{\bar{I}\bar{J}}}{2} |k\tau|^2 \\ -\frac{H^2 \mathcal{G}^{I\bar{J}}}{2} |k\tau|^2 & \frac{H^2 \mathcal{G}^{\bar{I}J}}{2} |k\tau|^4 \end{pmatrix} \quad (\text{B.7})$$

where $k\tau = -k/(aH)$. In our simulations, we impose these initial conditions 8 e-folds before the mode exits the horizon. Note that these initial conditions have corrections proportional to powers of ϵ_H (see around (3.9) of [167]). In our high-slope inflation models, ϵ_H is small at the time we impose these initial conditions.

In order to compute the physical gauge-invariant quantity ζ , the adiabatic perturbation on surfaces of constant density, we need to transform out of spatially flat gauge. The relevant transformation is [167]

$$N_a = \left(\frac{\pi_A}{2\epsilon_H}, 0 \right) \quad (\text{B.8})$$

where $\pi^A \equiv \partial_N \phi^A$. We can then define the ζ powerspectrum

$$P_\zeta(k, N) = \frac{1}{2\pi^2} N_a(N) N_b(N) \Sigma^{ab}(k, N) \quad (\text{B.9})$$

The scalar spectral index is then

$$n_s - 1 \equiv \frac{d \log P_\zeta}{d \log k} \quad (\text{B.10})$$

which we fit numerically, after solving for Σ^{ab} over a range of k -values. The isocurvature powerspectra are given by scalar fluctuations perpendicular to the adiabatic direction. We label a basis for these directions (i.e. the null space of N_A) as v_I^α , where α labels the $N_f - 1$ basis vectors and I labels the N_f vector components. We define the isocurvature powerspectra as

$$P_{\text{iso}}^{\alpha\beta} = \frac{1}{2\pi^2} \frac{1}{2\epsilon_H} v_I^\alpha(N) v_J^\beta(N) \Sigma^{IJ}(k, N) \quad (\text{B.11})$$

Note that we only index the field-field quadrant of the 2-point correlation matrix for this expression. The equivalent gauge transformation here is the $2\epsilon_H$ in the denominator. In practice, we often do not care about the individual isocurvature powerspectra, but only the total amount of isocurvature. This is given by the trace $P_{\text{iso}} \equiv \delta_{\alpha\beta} P_{\text{iso}}^{\alpha\beta}$.

Tensor perturbations can be treated similarly to the scalar ones. For a comprehensive treatment, we again refer the reader to [167]. In short, there is a two-component vector $Y_s^a = \{\gamma_s, \pi_s\}$, where γ_s is a scalar component of a tensor perturbation and $\pi_s \equiv \partial_N \gamma_s$ its momentum. The polarization is labelled by $s \in \{+, \times\}$. Their two-point function can be written

$$\langle Y_s^a(\vec{k}) Y_{s'}^b(\vec{k}') \rangle \equiv (2\pi)^3 \delta_{ss'} \delta(\vec{k} + \vec{k}') \Upsilon^{ab}(k) \quad (\text{B.12})$$

Similarly, we can evolve the dimensionless two-point function as

$$\partial_N \Upsilon^{ab} = w_c^a \Upsilon^{cb} + w_c^b \Upsilon^{ac} \quad (\text{B.13})$$

where

$$w_b^a \equiv \begin{pmatrix} 0 & 1 \\ -k^2/(aH)^2 & \epsilon_H - 3 \end{pmatrix}. \quad (\text{B.14})$$

The corresponding initial conditions are

$$\Upsilon^{ab}|_{\text{BD}} = H^2 \begin{pmatrix} |k\tau|^2 & -|k\tau|^2 \\ -|k\tau|^2 & |k\tau|^4 \end{pmatrix} \quad (\text{B.15})$$

At the end of inflation, the tensor amplitude at the pivot scale is $A_T = 4\Upsilon^{00}(k_\star, N_{\text{end}})/(2\pi^2)$, and the tensor-to-scalar ratio is $r \equiv A_T/P_\zeta(k_\star, N_{\text{end}})$.

C Derivation of Superpotential Model

Potentials of the form (4.3) lead to the equation:

$$\dot{\phi}^I = -2\mathcal{G}_{IJ} \frac{\partial W}{\partial \phi^J} \quad (\text{C.1})$$

In the two field case we considered in this paper where W only depends on X , this implies $\dot{Y} = 0$. In this Appendix we show that the converse is also true. We show that the potential

(4.3) may be obtained by examining $\dot{Y} = 0$ solutions to (2.1). Imposing this constraint, the equations of motion become

$$3H^2 = \frac{1}{2}e^{2Y/R_0}\dot{X}^2 + V \quad (\text{C.2})$$

$$\ddot{X} + 3H\dot{X} + e^{-2Y/R_0}\partial_X V = 0 \quad (\text{C.3})$$

$$-\frac{1}{R_0}e^{2Y/R_0}\dot{X}^2 + \partial_Y V = 0. \quad (\text{C.4})$$

Solving for \dot{X} and taking another time derivative, we obtain

$$\ddot{X} = \frac{R_0}{2}e^{-2Y/R_0}V_{YX}. \quad (\text{C.5})$$

Substituting into the Friedmann equation, we find

$$3H = \pm\sqrt{3}\sqrt{\frac{R_0}{2}V_Y + V}. \quad (\text{C.6})$$

The X equation of motion thus becomes

$$V_X + \frac{R_0}{2}V_{YX} = \pm\sqrt{3}e^{Y/R_0}\sqrt{V + \frac{R_0}{2}V_Y}\sqrt{R_0V_Y}, \quad (\text{C.7})$$

or

$$2\partial_X\left(\sqrt{V + \frac{R_0}{2}V_Y}\right) = \pm\sqrt{3R_0}e^{Y/R_0}\sqrt{V_Y}. \quad (\text{C.8})$$

Chen et al.'s solution arises from choosing a potential of the form $V(X, Y) = h(X) + f(X)g(Y)$. Equation (C.7) then becomes

$$h'(X) + f'(X)g(Y) + \frac{R_0}{2}f'(X)g'(Y) = \pm\sqrt{3R_0}e^{Y/R_0}\sqrt{h(X) + f(X)g(Y) + \frac{R_0}{2}f(X)g'(Y)} \\ \times \sqrt{f(X)g'(Y)}.$$

Choosing $g(Y) = -2e^{-2Y/R_0}$, this simplifies to

$$h'(X) = \pm\sqrt{12h(X)f(X)}. \quad (\text{C.9})$$

Defining $h(X) \equiv H^2(X)$ and $f(X) \equiv F^2(X)$, we see that

$$[H'(X)]^2 = 3F^2(X). \quad (\text{C.10})$$

For $W(X) \equiv \frac{H(X)}{\sqrt{3}}$, we recover the potential (4.3).

A separable potential, $V(X, Y) = f(X)g(Y)$, corresponds to taking $h(X) = 0$ above. Equation (C.7) becomes

$$\frac{f'(X)}{\pm\sqrt{3R_0}f(X)} = \sqrt{\frac{g'(Y)e^{2Y/R_0}}{g(Y) + \frac{R_0}{2}g'(Y)}} \equiv C, \quad (\text{C.11})$$

where C is a constant. Solving for f and g , we find

$$f(X) \propto e^{\pm\sqrt{3R_0}CX} \quad (\text{C.12})$$

$$g(Y) \propto \exp\left[\log(2e^{2Y/R_0} - R_0C^2) - \frac{2Y}{R_0}\right]. \quad (\text{C.13})$$

This yields

$$V(X, Y) = Be^{\pm\sqrt{3R_0C^2}X} \left(1 - \frac{R_0}{2}C^2e^{-2Y/R_0}\right), \quad (\text{C.14})$$

where B is a constant. Note that this separable potential is equivalent to the (4.3) with $W(X) = Ae^{X/R'}$, $R_0C^2 = \frac{4}{3(R')^2}$, and $B = 3A^2$.

D Derivation of Geodesics

For the field space with metric given in (4.1), we solve the geodesic equation:

$$(\phi'')^I + \Gamma_{JK}^I(\phi')^J(\phi')^K = 0 \quad (\text{D.1})$$

where λ parametrizes the geodesic and primes denote derivatives with respect to λ . Using the Christoffel symbols in (4.2), we obtain geodesic equations:

$$X'' + \frac{2}{R_0}X'Y' = 0 \quad (\text{D.2})$$

$$Y'' - \frac{1}{R_0}e^{2Y/R_0}(X')^2 = 0. \quad (\text{D.3})$$

The X equation can be expressed as:

$$\partial_\lambda \left(X'e^{2Y/R_0}\right) = 0 \quad \Rightarrow \quad X'e^{2Y/R_0} = C_1 \quad (\text{D.4})$$

where C_1 is a constant of integration. The Y equation then becomes:

$$Y'' - \frac{C_1^2}{R_0}e^{-2Y/R_0} = 0. \quad (\text{D.5})$$

This admits a solution of the form:

$$Y(\lambda) = R_0 \log \left[\frac{C_1^2 k_1 e^{\sqrt{k_1}(k_2+\lambda)/R_0} + e^{-\sqrt{k_1}(k_2+\lambda)/R_0}}{2k_1} \right], \quad (\text{D.6})$$

where k_1 and k_2 are constants of integration. Inserting this into the X equation, we have:

$$X' = C_1 \left[\frac{2k_1}{C_1^2 k_1 e^{\sqrt{k_1}(k_2+\lambda)/R_0} + e^{-\sqrt{k_1}(k_2+\lambda)/R_0}} \right]^2. \quad (\text{D.7})$$

This yields:

$$X(\lambda) = C - \frac{2\sqrt{k_1}R_0}{C_1} \frac{1}{C_1^2 k_1 e^{2\sqrt{k_1}(k_2+\lambda)/R_0} + 1}. \quad (\text{D.8})$$

Inverting this and using the solution for Y , we obtain:

$$Y(X) = R_0 \log \left[\frac{R_0}{(C - X) \sqrt{\frac{2\sqrt{k_1} R_0}{C_1(C-X)} - 1}} \right]. \quad (\text{D.9})$$

Defining $K = \frac{2\sqrt{k_1} R_0}{C_1}$, this simplifies to:

$$Y(X) = R_0 \log \left[\frac{R_0}{\sqrt{C - X} \sqrt{K - C + X}} \right]. \quad (\text{D.10})$$

The parameters C and K may be fixed such that the geodesic passes through any two points (X_1, Y_1) and (X_2, Y_2) such that $X_1 \neq X_2$; doing so yields

$$K = \sqrt{(X_2 - X_1)^2 + 2(Q_1 + Q_2) + \frac{(Q_2 - Q_1)^2}{(X_2 - X_1)^2}} \quad (\text{D.11})$$

$$C = \frac{1}{2} \left(X_2 + X_1 + \frac{Q_2 - Q_1}{X_2 - X_1} + K \right) \quad (\text{D.12})$$

$$Q_1 = R_0^2 e^{-2Y_1/R_0}, \quad Q_2 = R_0^2 e^{-2Y_2/R_0}. \quad (\text{D.13})$$

The geodesic distance between two points (X_i, Y_i) and (X_f, Y_f) is given by:

$$S = \int ds = \int_{X_i}^{X_f} \sqrt{e^{2Y/R_0} + \left(\frac{dY}{dX} \right)^2} dX. \quad (\text{D.14})$$

Integrating along the path given by (D.10), we have:

$$\begin{aligned} S &= \frac{R_0 K}{2} \int_{X_i}^{X_f} \frac{1}{(C - X)(C - K - X)} dX \\ &= \frac{R_0}{2} \log \left[\frac{C - X_f}{C - K - X_f} \frac{C - K - X_i}{C - X_i} \right]. \end{aligned} \quad (\text{D.15})$$

References

- [1] I.-S. Yang, *The Strong Multifield Slowroll Condition and Spiral Inflation*, *Phys. Rev.* **D85** (2012) 123532 [[1202.3388](#)].
- [2] A. Achúcarro and G. A. Palma, *The string swampland constraints require multi-field inflation*, [1807.04390](#).
- [3] A. R. Brown, *Hyperinflation*, [1705.03023](#).
- [4] E. J. Copeland, A. R. Liddle and J. E. Lidsey, *Steep inflation: Ending brane world inflation by gravitational particle production*, *Phys. Rev.* **D64** (2001) 023509 [[astro-ph/0006421](#)].
- [5] M. Sami, N. Dadhich and T. Shiromizu, *Steep inflation followed by Born-Infeld reheating*, *Phys. Lett.* **B568** (2003) 118 [[hep-th/0304187](#)].
- [6] M. M. Anber and L. Sorbo, *Naturally inflating on steep potentials through electromagnetic dissipation*, *Phys. Rev.* **D81** (2010) 043534 [[0908.4089](#)].

- [7] P. Adshead and M. Wyman, *Chromo-Natural Inflation: Natural inflation on a steep potential with classical non-Abelian gauge fields*, *Phys. Rev. Lett.* **108** (2012) 261302 [[1202.2366](#)].
- [8] M. M. Anber and L. Sorbo, *Non-Gaussianities and chiral gravitational waves in natural steep inflation*, *Phys. Rev.* **D85** (2012) 123537 [[1203.5849](#)].
- [9] K. Rezaeadeh, K. Karami and S. Hashemi, *Tachyon inflation with steep potentials*, *Phys. Rev.* **D95** (2017) 103506 [[1508.04760](#)].
- [10] P. Adshead, D. Blas, C. P. Burgess, P. Hayman and S. P. Patil, *Magnon Inflation: Slow Roll with Steep Potentials*, *JCAP* **1611** (2016) 009 [[1604.06048](#)].
- [11] K. Dimopoulos, *Steep Eternal Inflation and the Swampland*, *Phys. Rev.* **D98** (2018) 123516 [[1810.03438](#)].
- [12] D. Wands, *Multiple field inflation*, *Lect. Notes Phys.* **738** (2008) 275 [[astro-ph/0702187](#)].
- [13] S. Cremonini, Z. Lalak and K. Turzynski, *On Non-Canonical Kinetic Terms and the Tilt of the Power Spectrum*, *Phys. Rev.* **D82** (2010) 047301 [[1005.4347](#)].
- [14] S. Cremonini, Z. Lalak and K. Turzynski, *Strongly Coupled Perturbations in Two-Field Inflationary Models*, *JCAP* **1103** (2011) 016 [[1010.3021](#)].
- [15] A. Achucarro, J.-O. Gong, S. Hardeman, G. A. Palma and S. P. Patil, *Features of heavy physics in the CMB power spectrum*, *JCAP* **1101** (2011) 030 [[1010.3693](#)].
- [16] S. Renaux-Petel and K. Turzyński, *Geometrical Destabilization of Inflation*, *Phys. Rev. Lett.* **117** (2016) 141301 [[1510.01281](#)].
- [17] P. Agrawal, G. Obied, P. J. Steinhardt and C. Vafa, *On the Cosmological Implications of the String Swampland*, *Phys. Lett.* **B784** (2018) 271 [[1806.09718](#)].
- [18] G. Obied, H. Ooguri, L. Spodyneiko and C. Vafa, *De Sitter Space and the Swampland*, [1806.08362](#).
- [19] H. Ooguri, E. Palti, G. Shiu and C. Vafa, *Distance and de Sitter Conjectures on the Swampland*, [1810.05506](#).
- [20] S. K. Garg and C. Krishnan, *Bounds on Slow Roll and the de Sitter Swampland*, [1807.05193](#).
- [21] S. K. Garg, C. Krishnan and M. Z. Zaz, *Bounds on Slow Roll at the Boundary of the Landscape*, [1810.09406](#).
- [22] D. Andriot and C. Roupec, *Further refining the de Sitter swampland conjecture*, *Fortsch. Phys.* **67** (2019) 1800105 [[1811.08889](#)].
- [23] T. Rudelius, *Conditions for (No) Eternal Inflation*, [1905.05198](#).
- [24] S. Das, S. S. Haque and B. Underwood, *Constraints and Horizons for de Sitter with Extra Dimensions*, [1905.05864](#).
- [25] M. Benetti, S. Capozziello and L. L. Graef, *Swampland conjecture in $f(R)$ gravity by the Noether Symmetry Approach*, [1905.05654](#).
- [26] E. O. Colgáin and H. Yavartanoo, *Testing the Swampland: H_0 tension*, [1905.02555](#).
- [27] M. Sabir, W. Ahmed, Y. Gong, S. Hu and L. Wu, *A note on brane inflation under consistency conditions*, [1905.03033](#).
- [28] M. P. Rajvanshi and J. S. Bagla, *Reconstruction of Dynamical Dark Energy Potentials: Quintessence, Tachyon and interacting models*, [1905.01103](#).
- [29] N. Cabo Bizet, C. Damian, O. Loaiza-Brito and D. M. Peña, *Leaving the Swampland: Non-geometric fluxes and the Distance Conjecture*, [1904.11091](#).
- [30] A. Micu, *Two-field constant roll inflation*, [1904.10241](#).

- [31] A. Ijjas and P. J. Steinhardt, *A new kind of cyclic universe*, [1904.08022](#).
- [32] C. van de Bruck and C. C. Thomas, *Dark Energy, the Swampland and the Equivalence Principle*, [1904.07082](#).
- [33] S. Brahma and M. W. Hossain, *Relating the scalar weak gravity conjecture and the swampland distance conjecture for an accelerating universe*, [1904.05810](#).
- [34] U. Mukhopadhyay and D. Majumdar, *Swampland Criteria in Slotheon Field Dark Energy*, [1904.01455](#).
- [35] E. O. Colgáin, *Recasting H_0 tension as Ω_m tension at low z* , [1903.11743](#).
- [36] A. Slosar et al., *Dark Energy and Modified Gravity*, [1903.12016](#).
- [37] N. Kaloper, *Dark Energy, H_0 and Weak Gravity Conjecture*, [1903.11676](#).
- [38] E. Gonzalo and L. E. Ibáñez, *A Strong Scalar Weak Gravity Conjecture and Some Implications*, [1903.08878](#).
- [39] M. Sabir, W. Ahmed, Y. Gong and Y. Lu, *Superconformal attractor E-models in brane inflation under swampland criteria*, [1903.08435](#).
- [40] F. Farakos, *Runaway potentials and a massive goldstino*, [1903.07560](#).
- [41] P. Christodoulidis, D. Roest and E. I. Sfakianakis, *Scaling attractors in multi-field inflation*, [1903.06116](#).
- [42] S. Brahma and M. W. Hossain, *Dark energy beyond quintessence: Constraints from the swampland*, [1902.11014](#).
- [43] T. Bjorkmo, *The rapid-turn inflationary attractor*, [1902.10529](#).
- [44] P. Berglund, T. Hübsch and D. Minic, *On Stringy de Sitter Spacetimes*, [1902.08617](#).
- [45] J. P. Beltrán Almeida, A. Guarnizo, R. Kase, S. Tsujikawa and C. A. Valenzuela-Toledo, *Anisotropic 2-form dark energy*, [1902.05846](#).
- [46] M. Lynker and R. Schimmrigk, *Modular Inflation at Higher Level N* , [1902.04625](#).
- [47] S. Kadir, M. Lynker and R. Schimmrigk, *String Modular Phases in Calabi-Yau Families*, *J. Geom. Phys.* **61** (2011) 2453 [[1012.5807](#)].
- [48] L. Heisenberg, M. Bartelmann, R. Brandenberger and A. Refregier, *Horndeski in the Swampland*, [1902.03939](#).
- [49] J. Fumagalli, S. Garcia-Saenz, L. Pinol, S. Renaux-Petel and J. Ronayne, *Hyper non-Gaussianities in inflation with strongly non-geodesic motion*, [1902.03221](#).
- [50] M. Artymowski and I. Ben-Dayan, *$f(R)$ and Brans-Dicke Theories and the Swampland*, [1902.02849](#).
- [51] F. Carta, J. Moritz and A. Westphal, *Gaugino condensation and small uplifts in KKLT*, [1902.01412](#).
- [52] V. Kamali, *Reheating After Swampland Conjecture*, [1902.00701](#).
- [53] Y. Nan, K. Yamamoto, H. Aoki, S. Iso and D. Yamauchi, *Large-scale inhomogeneity of dark energy produced in the ancestor vacuum*, [1901.11181](#).
- [54] J. J. Heckman, C. Lawrie, L. Lin, J. Sakstein and G. Zoccarato, *Pixelated Dark Energy*, [1901.10489](#).
- [55] S. F. Bramberger and J.-L. Lehners, *Non-Singular Bounces Catalysed by Dark Energy*, [1901.10198](#).
- [56] D. Chway, *Light Bending in Models with a Generic Scalar Field*, [1901.09760](#).

- [57] T. Bjorkmo and M. C. D. Marsh, *Hyperinflation generalised: from its attractor mechanism to its tension with the ‘swampland conjectures’*, [1901.08603](#).
- [58] A. Kobakhidze, *A brief remark on convexity of effective potentials and de Sitter Swampland conjectures*, [1901.08137](#).
- [59] A. Achúcarro, E. J. Copeland, O. Iarygina, G. A. Palma, D.-G. Wang and Y. Welling, *Shift-Symmetric Orbital Inflation: single field or multi-field?*, [1901.03657](#).
- [60] V. Kamali, *Warm (Pseudo)Scalar Inflation*, [1901.01897](#).
- [61] P. Draper and S. Farkas, *Gravitational Instabilities and Censorship of Large Scalar Field Excursions*, [1901.00515](#).
- [62] G. Arciniega, P. Bueno, P. A. Cano, J. D. Edelstein, R. A. Hennigar and L. G. Jaime, *Geometric Inflation*, [1812.11187](#).
- [63] E. Belgacem, A. Finke, A. Frassino and M. Maggiore, *Testing nonlocal gravity with Lunar Laser Ranging*, *JCAP* **1902** (2019) 035 [[1812.11181](#)].
- [64] R.-G. Cai, S. Khimphun, B.-H. Lee, S. Sun, G. Tumurtushaa and Y.-L. Zhang, *Emergent Dark Universe and the Swampland Criteria*, [1812.11105](#).
- [65] M. Raveri, W. Hu and S. Sethi, *Swampland Conjectures and Late-Time Cosmology*, *Phys. Rev.* **D99** (2019) 083518 [[1812.10448](#)].
- [66] T. Coudarchet, L. Heurtier and H. Partouche, *Spontaneous dark-matter mass generation along cosmological attractors in string theory*, *JHEP* **03** (2019) 117 [[1812.10134](#)].
- [67] S. Abel, E. Dudas, D. Lewis and H. Partouche, *Stability and vacuum energy in open string models with broken supersymmetry*, [1812.09714](#).
- [68] P. Brax, P. Valageas and P. Vanhove, *Dark R^2 at low energy*, *Int. J. Mod. Phys.* **A33** (2018) 1845006.
- [69] M.-S. Seo, *de Sitter swampland bound in the Dirac-Born-Infeld inflation model*, *Phys. Rev.* **D99** (2019) 106004 [[1812.07670](#)].
- [70] M. Scalisi and I. Valenzuela, *Swampland Distance Conjecture, Inflation and α -attractors*, [1812.07558](#).
- [71] M. Bastero-Gil, A. Berera, R. Hernández-Jiménez and J. a. G. Rosa, *Warm inflation within a supersymmetric distributed mass model*, [1812.07296](#).
- [72] A. Bhardwaj, E. J. Copeland and J. Louko, *Inflation in Loop Quantum Cosmology*, *Phys. Rev.* **D99** (2019) 063520 [[1812.06841](#)].
- [73] E. Gonzalo, L. E. Ibáñez and A. M. Uranga, *Modular Symmetries and the Swampland Conjectures*, [1812.06520](#).
- [74] W.-C. Lin and W. H. Kinney, *Consistency of Tachyacoustic Cosmology with de Sitter Swampland Conjectures*, [1812.04447](#).
- [75] M. Montero, *A Holographic Derivation of the Weak Gravity Conjecture*, *JHEP* **03** (2019) 157 [[1812.03978](#)].
- [76] L. Heisenberg, H. Ramírez and S. Tsujikawa, *Inflation with mixed helicities and its observational imprint on CMB*, *Phys. Rev.* **D99** (2019) 023505 [[1812.03340](#)].
- [77] M. P. Hertzberg, M. Sandora and M. Trodden, *Quantum Fine-Tuning in Stringy Quintessence Models*, [1812.03184](#).
- [78] W. H. Kinney, *Eternal Inflation and the Refined Swampland Conjecture*, *Phys. Rev. Lett.* **122** (2019) 081302 [[1811.11698](#)].

- [79] Q. Bonnefoy, E. Dudas and S. Lüist, *On the weak gravity conjecture in string theory with broken supersymmetry*, [1811.11199](#).
- [80] C. A. R. Herdeiro, E. Radu and K. Uzawa, *Compact objects and the swampland*, *JHEP* **01** (2019) 215 [[1811.10844](#)].
- [81] B. S. Acharya, A. Maharana and F. Muia, *Hidden Sectors in String Theory: Kinetic Mixings, Fifth Forces and Quintessence*, *JHEP* **03** (2019) 048 [[1811.10633](#)].
- [82] A. Banlaki, A. Chowdhury, C. Roupec and T. Wrase, *Scaling limits of dS vacua and the swampland*, *JHEP* **03** (2019) 065 [[1811.07880](#)].
- [83] M. Emelin and R. Tatar, *Axion Hilltops, Kahler Modulus Quintessence and the Swampland Criteria*, [1811.07378](#).
- [84] R. Holman and B. Richard, *A Spinodal Solution to Swampland Inflationary Constraints*, [1811.06021](#).
- [85] F. Tosone, B. S. Haridasu, V. V. Luković and N. Vittorio, *Constraints on field flows of quintessence dark energy*, *Phys. Rev.* **D99** (2019) 043503 [[1811.05434](#)].
- [86] E. Elizalde and M. Khurshudyan, *Swampland criteria for a dark-energy dominated universe, ensuing from Gaussian process and $H(z)$ data analysis*, [1811.03861](#).
- [87] D. Y. Cheong, S. M. Lee and S. C. Park, *Higgs Inflation and the Refined dS Conjecture*, *Phys. Lett.* **B789** (2019) 336 [[1811.03622](#)].
- [88] R. I. Thompson, *Beta function quintessence cosmological parameters and fundamental constants – II. Exponential and logarithmic dark energy potentials*, *Mon. Not. Roy. Astron. Soc.* **482** (2019) 5448 [[1811.03164](#)].
- [89] C.-I. Chiang, J. M. Leedom and H. Murayama, *What does Inflation say about Dark Energy given the Swampland Conjectures?*, [1811.01987](#).
- [90] J. J. Heckman, C. Lawrie, L. Lin and G. Zoccarato, *F-theory and Dark Energy*, [1811.01959](#).
- [91] Z. Yi and Y. Gong, *Gauss-Bonnet inflation and swampland*, [1811.01625](#).
- [92] P. Agrawal and G. Obied, *Dark Energy and the Refined de Sitter Conjecture*, [1811.00554](#).
- [93] K. K. Kim, S. Koh and H. S. Yang, *Expanding Universe and Dynamical Compactification Using Yang-Mills Instantons*, *JHEP* **12** (2018) 085 [[1810.12291](#)].
- [94] C.-M. Lin, *Type I Hilltop Inflation and the Refined Swampland Criteria*, *Phys. Rev.* **D99** (2019) 023519 [[1810.11992](#)].
- [95] R. Schimmrigk, *The Swampland Spectrum Conjecture in Inflation*, [1810.11699](#).
- [96] G. Dvali, C. Gomez and S. Zell, *Quantum Breaking Bound on de Sitter and Swampland*, *Fortsch. Phys.* **67** (2019) 1800094 [[1810.11002](#)].
- [97] A. Hebecker and T. Wrase, *The Asymptotic dS Swampland Conjecture - a Simplified Derivation and a Potential Loophole*, *Fortsch. Phys.* **67** (2019) 1800097 [[1810.08182](#)].
- [98] H. Fukuda, R. Saito, S. Shirai and M. Yamazaki, *Phenomenological Consequences of the Refined Swampland Conjecture*, *Phys. Rev.* **D99** (2019) 083520 [[1810.06532](#)].
- [99] S.-J. Wang, *Electroweak relaxation of cosmological hierarchy*, *Phys. Rev.* **D99** (2019) 023529 [[1810.06445](#)].
- [100] S. Das, *Warm Inflation in the light of Swampland Criteria*, *Phys. Rev.* **D99** (2019) 063514 [[1810.05038](#)].
- [101] I. Antoniadis, Y. Chen and G. K. Leontaris, *Inflation from the internal volume in type IIB/F-theory compactification*, *Int. J. Mod. Phys.* **A34** (2019) 1950042 [[1810.05060](#)].

- [102] A. Ashoorioon, *Rescuing Single Field Inflation from the Swampland*, *Phys. Lett.* **B790** (2019) 568 [[1810.04001](#)].
- [103] S. D. Odintsov and V. K. Oikonomou, *Finite-time Singularities in Swampland-related Dark Energy Models*, [1810.03575](#).
- [104] M. Motaharfar, V. Kamali and R. O. Ramos, *Warm inflation as a way out of the swampland*, *Phys. Rev.* **D99** (2019) 063513 [[1810.02816](#)].
- [105] M. Kawasaki and V. Takhistov, *Primordial Black Holes and the String Swampland*, *Phys. Rev.* **D98** (2018) 123514 [[1810.02547](#)].
- [106] K. Hamaguchi, M. Ibe and T. Moroi, *The swampland conjecture and the Higgs expectation value*, *JHEP* **12** (2018) 023 [[1810.02095](#)].
- [107] C.-M. Lin, K.-W. Ng and K. Cheung, *Chaotic inflation on the brane and the Swampland Criteria*, [1810.01644](#).
- [108] P. Draper, *Virtual and Thermal Schwinger Processes*, *Phys. Rev.* **D98** (2018) 125014 [[1809.10768](#)].
- [109] D. Benisty and E. I. Guendelman, *Two scalar fields inflation from scale-invariant gravity with modified measure*, *Class. Quant. Grav.* **36** (2019) 095001 [[1809.09866](#)].
- [110] H. Matsui, F. Takahashi and M. Yamada, *Isocurvature Perturbations of Dark Energy and Dark Matter from the Swampland Conjecture*, *Phys. Lett.* **B789** (2019) 387 [[1809.07286](#)].
- [111] L. Visinelli and S. Vagnozzi, *Cosmological window onto the string axiverse and the supersymmetry breaking scale*, *Phys. Rev.* **D99** (2019) 063517 [[1809.06382](#)].
- [112] C. Han, S. Pi and M. Sasaki, *Quintessence Saves Higgs Instability*, *Phys. Lett.* **B791** (2019) 314 [[1809.05507](#)].
- [113] G. D'Amico, N. Kaloper and A. Lawrence, *Strongly Coupled Quintessence*, [1809.05109](#).
- [114] R. H. Brandenberger, *Beyond Standard Inflationary Cosmology*, [1809.04926](#).
- [115] D. Wang, *The multi-feature universe: large parameter space cosmology and the swampland*, [1809.04854](#).
- [116] U. Danielsson, *The quantum swampland*, *JHEP* **04** (2019) 095 [[1809.04512](#)].
- [117] S. Das, *Note on single-field inflation and the swampland criteria*, *Phys. Rev.* **D99** (2019) 083510 [[1809.03962](#)].
- [118] J. Quintin, R. H. Brandenberger, M. Gasperini and G. Veneziano, *Stringy black-hole gas in α' -corrected dilaton gravity*, *Phys. Rev.* **D98** (2018) 103519 [[1809.01658](#)].
- [119] R. J. Van Den Hoogen, A. A. Coley, B. Alhulaimi, S. Mohandas, E. Knighton and S. O'Neil, *Kantowski-Sachs Einstein-Aether Scalar Field Cosmological Models*, *JCAP* **1811** (2018) 017 [[1809.01458](#)].
- [120] K. Choi, D. Chway and C. S. Shin, *The dS swampland conjecture with the electroweak symmetry and QCD chiral symmetry breaking*, *JHEP* **11** (2018) 142 [[1809.01475](#)].
- [121] S. Brahma and M. Wali Hossain, *Avoiding the string swampland in single-field inflation: Excited initial states*, *JHEP* **03** (2019) 006 [[1809.01277](#)].
- [122] M. C. David Marsh, *The Swampland, Quintessence and the Vacuum Energy*, *Phys. Lett.* **B789** (2019) 639 [[1809.00726](#)].
- [123] H. Murayama, M. Yamazaki and T. T. Yanagida, *Do We Live in the Swampland?*, *JHEP* **12** (2018) 032 [[1809.00478](#)].
- [124] L. Heisenberg, M. Bartelmann, R. Brandenberger and A. Refregier, *Dark Energy in the Swampland II*, *Sci. China Phys. Mech. Astron.* **62** (2019) 990421 [[1809.00154](#)].

- [125] Y. Akrami, R. Kallosh, A. Linde and V. Vardanyan, *The Landscape, the Swampland and the Era of Precision Cosmology*, *Fortsch. Phys.* **67** (2019) 1800075 [[1808.09440](#)].
- [126] M. Cicoli, S. De Alwis, A. Maharana, F. Muia and F. Quevedo, *De Sitter vs Quintessence in String Theory*, *Fortsch. Phys.* **67** (2019) 1800079 [[1808.08967](#)].
- [127] A. del Rio, R. Durrer and S. P. Patil, *Tensor Bounds on the Hidden Universe*, *JHEP* **12** (2018) 094 [[1808.09282](#)].
- [128] K. Dasgupta, M. Emelin, E. McDonough and R. Tatar, *Quantum Corrections and the de Sitter Swampland Conjecture*, *JHEP* **01** (2019) 145 [[1808.07498](#)].
- [129] K. Dutta, Ruchika, A. Roy, A. A. Sen and M. M. Sheikh-Jabbari, *Beyond Λ CDM with Low and High Redshift Data: Implications for Dark Energy*, [1808.06623](#).
- [130] W. H. Kinney, S. Vagnozzi and L. Visinelli, *The zoo plot meets the swampland: mutual (in)consistency of single-field inflation, string conjectures, and cosmological data*, [1808.06424](#).
- [131] B.-M. Gu and R. Brandenberger, *Reheating and Entropy Perturbations in Fibre Inflation*, [1808.03393](#).
- [132] C. Damian and O. Loaiza-Brito, *Two-Field Axion Inflation and the Swampland Constraint in the Flux-Scaling Scenario*, *Fortsch. Phys.* **67** (2019) 1800072 [[1808.03397](#)].
- [133] L. Heisenberg, M. Bartelmann, R. Brandenberger and A. Refregier, *Dark Energy in the Swampland*, *Phys. Rev.* **D98** (2018) 123502 [[1808.02877](#)].
- [134] C.-I. Chiang and H. Murayama, *Building Supergravity Quintessence Model*, [1808.02279](#).
- [135] I. Ben-Dayan, *Draining the Swampland*, [1808.01615](#).
- [136] H. Matsui and F. Takahashi, *Eternal Inflation and Swampland Conjectures*, *Phys. Rev.* **D99** (2019) 023533 [[1807.11938](#)].
- [137] D. Andriot, *New constraints on classical de Sitter: flirting with the swampland*, *Fortsch. Phys.* **67** (2019) 1800103 [[1807.09698](#)].
- [138] C. Roupec and T. Wrase, *de Sitter Extrema and the Swampland*, *Fortsch. Phys.* **67** (2019) 1800082 [[1807.09538](#)].
- [139] A. Ghalee, *Condensation of a scalar field non-minimally coupled to gravity in a cosmological context*, [1807.08620](#).
- [140] S. Paban and R. Rosati, *Inflation in Multi-field Modified DBI Potentials*, *JCAP* **1809** (2018) 042 [[1807.07654](#)].
- [141] E. Ó Colgáin, M. H. P. M. van Putten and H. Yavartanoo, *de Sitter Swampland, H_0 tension & observation*, *Phys. Lett.* **B793** (2019) 126 [[1807.07451](#)].
- [142] F. Denef, A. Hebecker and T. Wrase, *de Sitter swampland conjecture and the Higgs potential*, *Phys. Rev.* **D98** (2018) 086004 [[1807.06581](#)].
- [143] M. Dias, J. Frazer, A. Retolaza and A. Westphal, *Primordial Gravitational Waves and the Swampland*, *Fortsch. Phys.* **67** (2019) 2 [[1807.06579](#)].
- [144] S. Rasouli, K. Rezazadeh, A. Abdolmaleki and K. Karami, *Warm DBI inflation with constant sound speed*, *Eur. Phys. J.* **C79** (2019) 79 [[1807.05732](#)].
- [145] A. Kehagias and A. Riotto, *A note on Inflation and the Swampland*, *Fortsch. Phys.* **66** (2018) 1800052 [[1807.05445](#)].
- [146] J.-L. Lehners, *Small-Field and Scale-Free: Inflation and Ekpyrosis at their Extremes*, *JCAP* **1811** (2018) 001 [[1807.05240](#)].
- [147] K. Dimopoulos and T. Markkanen, *Dark energy as a remnant of inflation and electroweak symmetry breaking*, *JHEP* **01** (2019) 029 [[1807.04359](#)].

- [148] L. Aalsma, M. Tournoy, J. P. Van Der Schaar and B. Vercnocke, *Supersymmetric embedding of antibrane polarization*, *Phys. Rev.* **D98** (2018) 086019 [1807.03303].
- [149] L. Heisenberg, *A systematic approach to generalisations of General Relativity and their cosmological implications*, *Phys. Rept.* **796** (2019) 1 [1807.01725].
- [150] S. Banerjee, U. Danielsson, G. Dibitetto, S. Giri and M. Schillo, *Emergent de Sitter Cosmology from Decaying Anti-de Sitter Space*, *Phys. Rev. Lett.* **121** (2018) 261301 [1807.01570].
- [151] G. Dvali and C. Gomez, *On Exclusion of Positive Cosmological Constant*, *Fortsch. Phys.* **67** (2019) 1800092 [1806.10877].
- [152] D. Andriot, *On the de Sitter swampland criterion*, *Phys. Lett.* **B785** (2018) 570 [1806.10999].
- [153] P. Agrawal, J. Fan and M. Reece, *Clockwork Axions in Cosmology: Is Chromonatural Inflation Chrononatural?*, *JHEP* **10** (2018) 193 [1806.09621].
- [154] S. Vagnozzi, S. Dhawan, M. Gerbino, K. Freese, A. Goobar and O. Mena, *Constraints on the sum of the neutrino masses in dynamical dark energy models with $w(z) \geq -1$ are tighter than those obtained in Λ CDM*, *Phys. Rev.* **D98** (2018) 083501 [1801.08553].
- [155] L. Visinelli, *Light axion-like dark matter must be present during inflation*, *Phys. Rev.* **D96** (2017) 023013 [1703.08798].
- [156] S. Brahma and S. Shandera, *Stochastic eternal inflation is in the swampland*, 1904.10979.
- [157] S. Mizuno and S. Mukohyama, *Primordial perturbations from inflation with a hyperbolic field-space*, *Phys. Rev.* **D96** (2017) 103533 [1707.05125].
- [158] S. Renaux-Petel, K. Turzyński and V. Vennin, *Geometrical destabilization, premature end of inflation and Bayesian model selection*, *JCAP* **1711** (2017) 006 [1706.01835].
- [159] M. Cicoli, V. Guidetti, F. G. Pedro and G. P. Vacca, *A geometrical instability for ultra-light fields during inflation?*, *JCAP* **1812** (2018) 037 [1807.03818].
- [160] O. Grocholski, M. Kalinowski, M. Kolanowski, S. Renaux-Petel, K. Turzyński and V. Vennin, *On backreaction effects in geometrical destabilisation of inflation*, *JCAP* **1905** (2019) 008 [1901.10468].
- [161] T. Bjorkmo, R. Z. Ferreira and M. C. D. Marsh, *Mild Non-Gaussianities under Perturbative Control from Rapid-Turn Inflation Models*, *JCAP* **1912** (2019) 036 [1908.11316].
- [162] P. Christodoulidis, D. Roest and E. Sfakianakis, *Attractors, Bifurcations and Curvature in Multi-field Inflation*, 1903.03513.
- [163] D. I. Kaiser, E. A. Mazenc and E. I. Sfakianakis, *Primordial Bispectrum from Multifield Inflation with Nonminimal Couplings*, *Phys. Rev.* **D87** (2013) 064004 [1210.7487].
- [164] M. Berg, E. Pajer and S. Sjors, *Dante’s Inferno*, *Phys. Rev.* **D81** (2010) 103535 [0912.1341].
- [165] G. Barenboim and W.-I. Park, *Spiral Inflation*, *Phys. Lett.* **B741** (2015) 252 [1412.2724].
- [166] R. Feldt, “Blackboxoptim.jl.” <https://github.com/robertfeldt/BlackBoxOptim.jl>, 2019.
- [167] M. Dias, J. Frazer and D. Seery, *Computing observables in curved multifield models of inflation—A guide (with code) to the transport method*, *JCAP* **1512** (2015) 030 [1502.03125].
- [168] A. Achúcarro, J.-O. Gong, S. Hardeman, G. A. Palma and S. P. Patil, *Effective theories of single field inflation when heavy fields matter*, *JHEP* **05** (2012) 066 [1201.6342].
- [169] A. Achúcarro, V. Atal, S. Céspedes, J.-O. Gong, G. A. Palma and S. P. Patil, *Heavy fields, reduced speeds of sound and decoupling during inflation*, *Phys. Rev.* **D86** (2012) 121301 [1205.0710].

- [170] A. Hetz and G. A. Palma, *Sound Speed of Primordial Fluctuations in Supergravity Inflation*, *Phys. Rev. Lett.* **117** (2016) 101301 [[1601.05457](#)].
- [171] S. Céspedes and G. A. Palma, *Cosmic inflation in a landscape of heavy-fields*, *JCAP* **1310** (2013) 051 [[1303.4703](#)].
- [172] C. P. Burgess, M. W. Horbatsch and S. Patil, *Inflating in a Trough: Single-Field Effective Theory from Multiple-Field Curved Valleys*, *JHEP* **01** (2013) 133 [[1209.5701](#)].
- [173] PLANCK collaboration, *Planck 2018 results. X. Constraints on inflation*, [1807.06211](#).
- [174] PLANCK collaboration, *Planck 2018 results. IX. Constraints on primordial non-Gaussianity*, [1905.05697](#).
- [175] A. J. Tolley and M. Wyman, *The Gelaton Scenario: Equilateral non-Gaussianity from multi-field dynamics*, *Phys. Rev.* **D81** (2010) 043502 [[0910.1853](#)].
- [176] M. Hazumi et al., *LiteBIRD: A Satellite for the Studies of B-Mode Polarization and Inflation from Cosmic Background Radiation Detection*, *J. Low. Temp. Phys.* **194** (2019) 443.
- [177] X. Chen, G. A. Palma, W. Riquelme, B. Scheiding Hitschfeld and S. Sypsas, *Landscape tomography through primordial non-Gaussianity*, [1804.07315](#).
- [178] A. Achúcarro, V. Atal, C. Germani and G. A. Palma, *Cumulative effects in inflation with ultra-light entropy modes*, *JCAP* **1702** (2017) 013 [[1607.08609](#)].
- [179] S. Garcia-Saenz and S. Renaux-Petel, *Flattened non-Gaussianities from the effective field theory of inflation with imaginary speed of sound*, *JCAP* **1811** (2018) 005 [[1805.12563](#)].